AUV Navigation and Localization: A Review

Liam Paull, Sajad Saeedi, Mae Seto, and Howard Li

Abstract—Autonomous underwater vehicle (AUV) navigation and localization in underwater environments is particularly challenging due to the rapid attenuation of Global Positioning System (GPS) and radio-frequency signals. Underwater communications are low bandwidth and unreliable, and there is no access to a global positioning system. Past approaches to solve the AUV localization problem have employed expensive inertial sensors, used installed beacons in the region of interest, or required periodic surfacing of the AUV. While these methods are useful, their performance is fundamentally limited. Advances in underwater communications and the application of simultaneous localization and mapping (SLAM) technology to the underwater realm have yielded new possibilities in the field. This paper presents a review of the state of the art of AUV navigation and localization, as well as a description of some of the more commonly used methods. In addition, we highlight areas of future research potential.

Index Terms—Autonomous underwater vehicles (AUVs), marine navigation, simultaneous localization and mapping.

I. INTRODUCTION

THE development of autonomous underwater vehicles (AUVs) began in earnest in the 1970s. Since then, advancements in the efficiency, size, and memory capacity of computers have enhanced that potential. As a result, many tasks that were originally achieved with towed arrays or manned vehicles are being completely automated. AUV designs include torpedo-like, gliders, and hovering, and their sizes range from human portable to hundreds of tons.

AUVs are now being used for a variety of tasks, including oceanographic surveys, demining, and bathymetric data collection in marine and riverine environments. Accurate localization and navigation is essential to ensure the accuracy of the gathered data for these applications.

A distinction should be made between navigation and localization. Navigational accuracy is the precision with which the AUV guides itself from one point to another. Localization accuracy is the error in how well the AUV localizes itself within a map.

AUV navigation and localization is a challenging problem due primarily to the rapid attenuation of higher frequency signals and the unstructured nature of the undersea environment. Above water, most autonomous systems rely on radio or spread-spectrum communications and global positioning. However, underwater, such signals propagate only short distances and acoustic-based sensors and communications perform better. Acoustic communications still suffer from many shortcomings such as:

- small bandwidth, which means communicating nodes have had to use time-division multiple-access (TDMA) techniques to share information;
- low data rate, which generally constrains the amount of data that can be transmitted;
- high latency since the speed of sound in water is only 1500 m/s (slow compared with the speed of light);
- variable sound speed due to fluctuating water temperature and salinity;
- multipath transmissions due to the presence of an upper (free surface) and lower (sea bottom) boundary coupled with highly variable sound speed;
- unreliability, resulting in the need for a communication system designed to handle frequent data loss in transmissions.

Notwithstanding these significant challenges, research in AUV navigation and localization has exploded in the last ten years. The field is in the midst of a paradigm shift from old technologies, such as long baseline (LBL) and ultrashort baseline (USBL), which require predeployed and localized infrastructure, toward dynamic multiagent system approaches that allow for rapid deployment and flexibility with minimal infrastructure. In addition, simultaneous localization and mapping (SLAM) techniques developed for above ground robotics applications are being increasingly applied to underwater systems. The result is that bounded error and accurate navigation for AUVs is becoming possible with less cost and overhead.

A. Outline

AUV navigation and localization techniques can be categorized according to Fig. 1. This review paper will be organized based on this structure.

In general, these techniques fall into one of three main categories.

- Inertial/dead reckoning: Inertial navigation uses accelerometers and gyroscopes for increased accuracy to propagate the current state. Nevertheless, all of the methods in this category have position error growth that is unbounded.
- Acoustic transponders and modems: Techniques in this category are based on measuring the time of flight (TOF) of signals from acoustic beacons or modems to perform navigation.

L. Paull, S. Saeedi, and H. Li are with the Department of Electrical and Computer Engineering, University of New Brunswick, Fredericton, NB E3B 5A3 Canada (e-mail: liam.paull@unb.ca; sajad.saeedi.g@unb.ca; howard@unb.ca).
M. Seto is with the Defence Research and Development Canada, Dartmouth, NS B2Y 3Z7 Canada (e-mail: mae.seto@drdc-rddc.gc.ca).
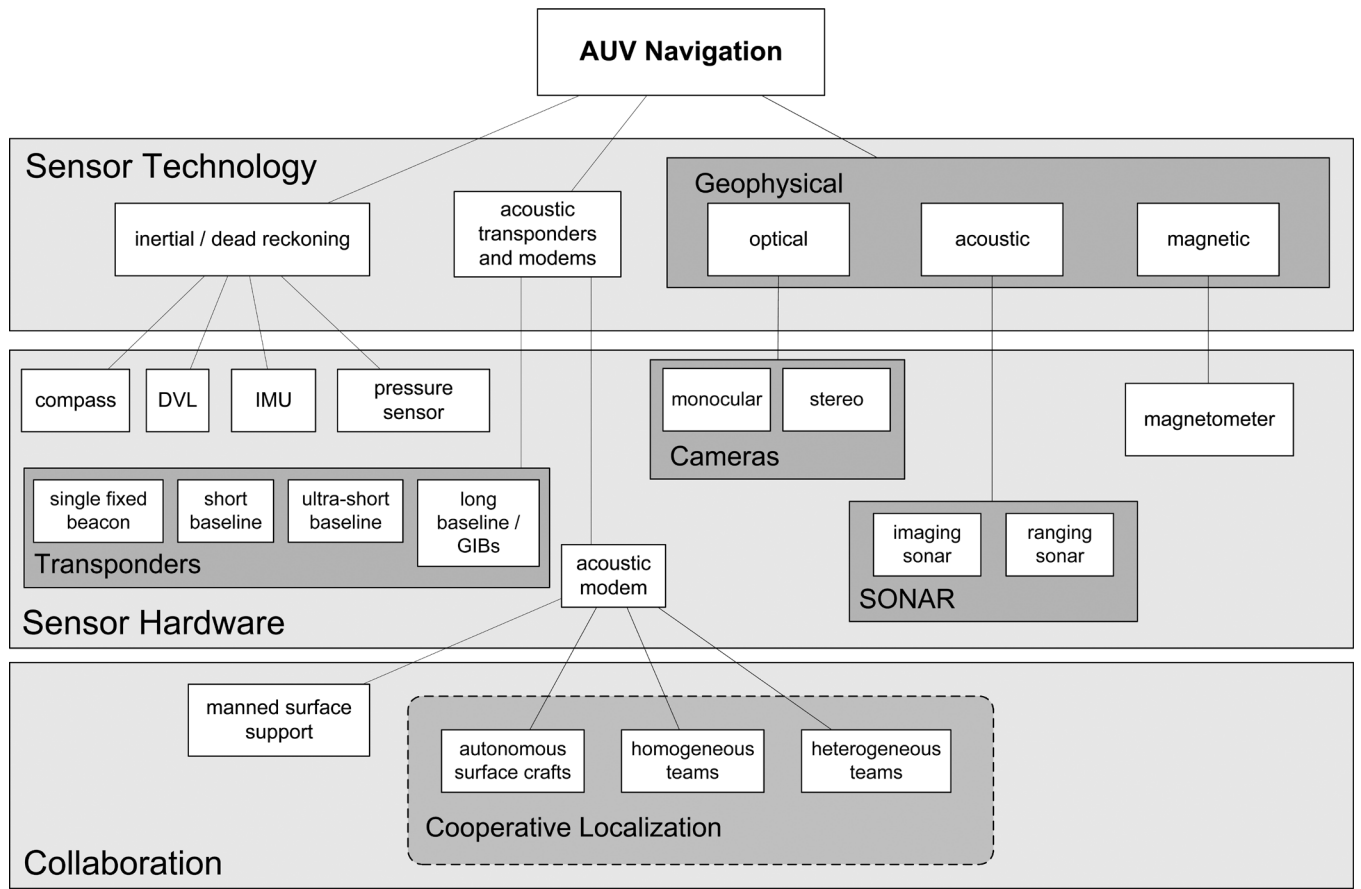
Fig. 1. Outline of underwater navigation classifications. These methods are often combined in one system to provide increased performance.

- Geophysical: Techniques that use external environmental information as references for navigation. This must be done with sensors and processing that are capable of detecting, identifying, and classifying some environmental features.

Sonar sensors are based on acoustic signals, however, navigation with imaging or bathymetric sonars are based on detection, identification, and classification of features in the environment. Therefore, navigation that is sonar based falls into both the acoustic and geophysical categories. A distinction is made between sonar and other acoustic-based navigation schemes, which rely on externally generated acoustic signals emitted from beacons or other vehicles.

The type of navigation system used is highly dependent on the type of operation or mission and that in many cases different systems can be combined to yield increased performance. The most important considerations are the size of the region of interest and the desired localization accuracy.

Past reviews on this topic include [1]–[3]. Significant advances have been made since these reviews both in previously established technologies, and in new areas. In particular, the development of acoustic communications through the use of underwater modems has led to the development of new algorithms. In addition, advancement in SLAM research has been applied to the underwater domain in a number of new ways.

II. BACKGROUND

Most modern systems process and filter the data from the sensors to derive a coherent, recursive estimate of the AUV pose.

This section will review some of the most common underwater sensors, popular state estimation filters, the basics of SLAM, and the foundations of cooperative navigation.

A. Commonly Used Underwater Navigation Sensors

Table I describes some commonly used sensors for underwater navigation.

B. State Estimation

The basis of any navigation algorithm is state estimation. Consider a robot whose pose at time t is given by x_t.

The goal of recursive state estimation is to estimate the belief distribution of the state x_t denoted by $\mathrm{bel}(x_t)$ given by

$$\mathrm{bel}(x_t) = p(x_t \mid u_{1:t}, z_{1:t}) \tag{1}$$

where u is some control input or odometry and z is a measurement used for localization.

The propagation of the state is given by some general nonlinear process equation

$$x_t = f(x_{t-1}, u_t, \epsilon_t) \tag{2}$$

where ϵ_t is the process noise. The state is observable through some measurement function

$$z_t = h(x_t, \delta_t) \tag{3}$$

TABLE I
SOME ONBOARD AUV SENSORS USED FOR STATE ESTIMATION

COMPASS

Description	Performance	Cost
A compass provides a globally bounded heading reference. A typical magnetic compass does so by measuring the magnetic field vector. This type of compass is subject to bias in the presence of objects with a strong magnetic signature and points to the earth's magnetic north pole. More common in marine applications, a gyrocompass measures heading using a fast spinning disc and the rotation of the earth. It is unaffected by metallic objects and points to true north.	Accuracy within 1° to 2° for a modestly priced unit.	On the order of hundreds of dollars US.

PRESSURE SENSOR

Description	Performance	Cost
Underwater depth can be measured with a barometer or pressure sensor.	Since the pressure gradient is much steeper underwater (10m = 1 atmosphere) we can achieve high accuracy $\approx$ 0.1m.	$\approx$ \$100 $-$ $200USD$

DOPPLER VELOCITY LOG

Description	Performance	Cost
The DVL uses acoustic measurements to capture bottom tracking and determine the velocity vector of an AUV moving across the seabed. It determines the AUV surge, sway, and heave velocities by transmitting acoustic pulses and measuring the Doppler shifted returns from these pulses off the seabed. DVLs will typically consist of 4 or more beams. 3 beams are needed to obtain a 3D velocity vector .	Nominal standard deviation on the order of 0.3cm/s-0.8cm/s.	$\approx$ \$20k - 80k USD

where δ_t is the measurement noise. Typically, the state at time t is recursively estimated through an approximation of the Bayes' filter which operates in a predict–update cycle. Prediction is given by [6]

$$\overline{\text{bel}}(x_t) = \sum_{x_{t-1}} p(x_t \mid x_{t-1}, u_t)\text{bel}(x_{t-1}) \qquad (4)$$

and update is given by

$$\text{bel}(x_t) = \eta p(z_t \mid x_t)\overline{\text{bel}}(x_t) \qquad (5)$$

where η is a normalization factor. Implicit in this formulation is the Markov assumption, which states that only the most recent state estimates, control, and measurements need to be considered to generate the estimate of the next state.

Some of the more popular state estimation algorithms are summarized in Table II. For further details, see, for example, [6].

All of the filters described in Table II have been used in AUV navigation algorithms that will be described in the following sections. Some implementations differ by what variables are maintained in the state space as relevant to the navigation problem. For example, tide level [8], water current [9], [10], the speed of sound in water [11], or inertial sensor drift [11] can all be estimated to improve navigation. There are also popular variants of these classical filters. For example, since acoustic propagations are relatively slow compared to radio-frequency communications it is often necessary to implement a delayed-state filter to account for the delay. Examples include [12], where a delayed state extended information filter (EIF) is used, and [13], which implements a delayed-state extended Kalman filter (EKF).

Often state estimation is decomposed into two parts: the attitude heading and reference system (AHRS) and the inertial navigation system (INS), as shown in Fig. 2. All sensors that give information about Euler angles or rates are inputs into the AHRS, which produces a stable estimate of vehicle orientation. The stabilized roll, pitch, and yaw are then used by the INS in combination with other sensors that give information about vehicle position, linear velocity, or linear acceleration to estimate the vehicle position.

C. Simultaneous Localization and Mapping

SLAM is the process of a robot autonomously building a map of its environment and, at the same time, localizing itself within that environment.[1] SLAM algorithms can be either *online*, where only the current pose is estimated along with the map, or *full* where the posterior is calculated over the entire robot trajectory [6]. Analytically, online SLAM involves estimating the posterior over the momentary pose x_t and the map m, given all measurements $z_{1:t}$ and inputs $u_{1:t}$

$$p(x_t, m \mid z_{1:t}, u_{1:t}) \qquad (6)$$

whereas full SLAM involves estimating the posterior over the entire pose trajectory

$$p(x_{1:t}, m \mid z_{1:t}, u_{1:t}). \qquad (7)$$

In addition, SLAM implementations can be classified as *feature based*, where features are extracted (detection, identification, and classification) and maintained in the state space, or

[1]Also referred to as concurrent mapping and localization.

view based, where poses corresponding to measurements are maintained in the state space.

As Fig. 3(a) shows, in feature-based SLAM, features are extracted from sensor measurements. For example, at pose P_1, the robot sees three features L_1, L_2, and L_3. These features together with the pose of the robot are maintained in the state space. At the next pose P_2, only newly observed features L_4 and L_5 are added to the vector and the pose is replaced with the previous pose. This process occurs at each new pose. In view-based SLAM [Fig. 3(b)], at each pose the whole view without extracting any features is processed, usually by comparing it with the previous view. For example, at pose P_3, V_3 is compared with V_2 to find the view-based odometry. State vectors in this case can be composed by one or more of the poses at each time.

Filtering (online) approaches to SLAM make use of a state estimation algorithm such as those presented in Table II. Smoothing (full SLAM) methods, also known as GraphSLAM [33], minimize the process and observation constraints over the whole trajectory of the robot. Some approaches use a combination of methods.

Some of the most popular categories of SLAM approaches are described here with their pros, cons, and AUV navigation references provided in Table III. The categorization is based on [6] with some additions.

- EKF–SLAM: It linearizes the system model using the Taylor expansion. It applies recursive predict–update cycle to estimate pose and map. Its state vector includes pose and features [14]. It is applicable to both view-based SLAM [37] and feature-based SLAM [38]. For large maps, EKF–SLAM is computationally expensive since computation time scales $\mathcal{O}(n^2)$ where n is the number of features.

- SEIF–SLAM: Sparse extended information filter (SEIF) [23] and exactly sparse extended information filter (ESEIF) [39] are two well-known approaches for SLAM using the information filter. They both maintain a sparse information matrix which preserves the consistency of the Gaussian distribution; however, accessing the mean and covariance requires a computationally expensive large matrix inversion. Both approaches need the information matrix to be actively "sparsified" by a sparsification strategy. ESEIF maintains an information matrix with the majority of elements being *exactly* zero which avoids the overconfidence problem of [23].

- FastSLAM: It is based on the particle filter. Particle filtering approaches are nonlinear filtering solutions; therefore, the system models are not approximated. In FastSLAM, poses and features are represented by particles (points) in the state space [27]. FastSLAM is the only solution which performs online SLAM and full SLAM together, which means it estimates not only the current pose, but also the full trajectory. In FastSLAM, each particle holds an estimate of the pose and all features; however, each feature is represented and updated through a separate EKF. Similar to other methods, it is applicable to both view-based SLAM [40] and feature-based SLAM [6].

- GraphSLAM: In GraphSLAM methods, the entire trajectory and map are estimated [33]. GraphSLAM also uses ap-

proximation by Taylor expansion, however, it differs from EKF–SLAM in that it accumulates information and, therefore, is considered to be an offline algorithm [6]. Generally, in GraphSLAM, poses of the robot are represented as nodes in a graph. The edges connecting nodes are modeled with motion and observation constraints. These constraints need to be optimized to calculate the spatial distribution of the nodes and their uncertainties [6]. Different solutions exist for GrpahSLAM, such as relaxation on a mesh [41], multilevel relaxation [42], iterative alignment [43], square root smoothing and mapping (SAM) [7], incremental smoothing and mapping (iSAM) [44] and works by Grisetti *et al.* [45], [46], and hierarchical optimization for pose graphs on manifolds (HOGMAN) [47]. In principle, they are all similar, but differ in how the optimization is implemented. For instance, iSAM solves the full SLAM problem by updating a matrix factorization while HOGMAN's optimization is performed over a manifold.

- Artificial intelligence (AI) SLAM: These methods of SLAM are based on fuzzy logic and neural networks. ratSLAM [48] is a technique that models rodents' brain using neural networks. In fact, this method is neural-network-based data fusion using a camera and an odometer. Saeedi *et al.* [49] use self-organizing maps (SOMs) to perform SLAM with multiple robots. The SOM is a neural network which is trained without supervision.

The choice of the method for estimating the poses of robots and the map depends on many factors, such as the available memory, processing capability, and type of sensory information.

SLAM techniques have been used for acoustic (Section IV) and particularly geophysical (Section V) underwater navigation algorithms, as will be described.

D. Cooperative Navigation

In cooperative navigation (CN), AUV teams localize using proprioceptive sensors as well as communication updates from other team members.

CN finds its origin in ground robotics applications. In the seminal paper by Roumeliotis and Bekey [50], it is proven that a group of autonomous agents with no access to global positioning can localize themselves more accurately if they can share pose estimates and uncertainty as well as make relative measurements. In [51], the scalability of CN is addressed, and it is shown that an upper bound on the rate of increase of position uncertainty is a function of the size of the robot team. Other important results have been proven, such as that the maximum expected rate of uncertainty increase is independent of the accuracy and number of intervehicle measurements and depends only on the accuracy of the proprioceptive sensors on the robots [52]. In addition, applications of maximum *a posteriori* [53], [54], EKF [55], and nonlinear least squares [56] estimators have been developed for general robotics CN. A complexity analysis is also presented in [57]. Special considerations must be made to apply many of these algorithms to underwater CN since the acoustic communication channel is limited. Further detail will be presented in Section IV.

TABLE I
(*CONTINUED.*) SOME ONBOARD AUV SENSORS USED FOR STATE ESTIMATION

SONAR

Description	Performance	Cost
A sonar is a device for remotely detecting and locating objects in water using sound. Passive sonars are listening devices that record the sounds emitted by objects in water. Active sonars are devices that produce sound waves of specific, controlled frequencies, and listen for the echoes of these emitted sounds returned from remote objects in the water. Active sonars can be categorized as either imaging sonars that produce an image of the seabed, or ranging sonars which produce bathymetric maps. More details of specific active sonar devices are presented in Table IV in Sec. V-B.	Along-track image resolution for an imaging side-scan sonar is a function of many factors such as range, sonar frequency, and water conditions, however cross-track resolution is independent of range. For example, a Klein 5000 side-scan operating at 455kHz can achieve an along track resolution of 10cm at 38m range and 61cm at the maximum 250m range and a Klein 5900 sidescan operating at 600kHz can achieve along track resolution 5cm at 10m and 20cm resolution at the maximum 100m range. In both cases nominal cross-track resolution is 3.75cm Resolution for a bathymetry sonar is on the order of $\approx 0.4^o - 2^o$ along track and $\approx 5 - 10$cm cross track [4].	Prices vary widely from $20k - 200kUSD$ or more. [4]

GLOBAL POSITIONING SYSTEM

Description	Performance	Cost
Global Positioning Systems can be used for surface vehicles. Position is estimated using the time-of-flight of signals from synchronized satellites.	Many factors can influence the accuracy of a GPS reading, including type of GPS technique used, atmospheric conditions, number of satellites in view, and others. Precisions for different GPS systems are: common commercial off-the-shelf GPS - 10m, Wide Area Differential GPS (WADGPS) - 0.3-2m, Real-Time Kinematic (RTK) - 0.05-0.5m, Post processed - 0.02 - 0.25m.	From hundreds to thousands of dollars.

TABLE I
(*CONTINUED.*) SOME ONBOARD AUV SENSORS USED FOR STATE ESTIMATION

INERTIAL MEASUREMENT UNIT

Description	Performance	Cost

Use a combination of accelerometers and gyroscopes (and sometimes magnetometers) to estimate a vehicle's orientation, velocity, and gravitational forces.
 • Gyroscope: Measures angular rates. For underwater applications, the following two categories are widely used:
  – Ring Laser / Fibre Optic: Light is passed either through a series of mirrors (ring laser) or fibre optic cable in different directions. The angular rates are determined based on the phase change of the light after passing through the mirrors or fibre.
  – MEMS: An oscillating mass is suspended within a spring system. Rotation of the gyroscope results in a perpendicular Coriolis force on the mass which can be used to calculate the angular rate of sensor.
 Since a gyroscope measures angular rates, there will be a drift in the estimated Euler angles as a result of integration.
 • Accelerometer: Measures the force required to accelerate a proof mass. Common designs include pendulum, MEMS, and vibrating beam among others.
	Gyroscope - Drift extremely variable from $0.0001^o/hr$ (RLG) to $60^o/hr$ or more for MEMS [5]. Accelerometer - Bias range from $0.01mg$ (MEMS) to $0.001mg$ (Pendulum) [5].	Extremely variable. From hundreds of dollars for a MEMS IMU to hundreds of thousands of dollars for a commercial grade ringlaser or fibre optic system.

A graphical depiction of multiple AUV CN is shown in Fig. 4. Data are transmitted through the acoustic channel. Upon reception of a data packet, the receiver, vehicle j, can use the TOF of the acoustic signal to determine its range R_{ij} from the sender, vehicle i. If the vehicles possess well-synchronized clocks, then this range can be determined from the one-way travel time (OWTT) of the acoustic signal, otherwise an interrogation reply is performed to determine a round-trip range (RTR).

TABLE II
SOME COMMON STATE ESTIMATION TECHNIQUES

| State Estimator	Description
Bayes' Filter	Optimal but computationally intractable for all but the simplest of estimation problems.
Kalman Filter (KF)	State distribution assumed to be Gaussian and parameterized by mean, μ, and covariance, Σ. Requires (2) and (3) to be linear. Optimal conditional on Gaussian and linearity assumptions.
Extended Kalman Filter (EKF)	Extension of the Kalman filter to accommodate non-linear process and measurement models. On each iteration, (2) and (3) are linearized about the mean. Prediction operation is fast, but measurement update is slow as it requires matrix inversion.
Unscented Kalman Filter (UKF)	Reduces the linearization errors of the EKF at the expense of higher computation. Instead of just mean and covariance being mapped through the non-linear functions, multiple 'sigma' points are mapped and then the output is re-parameterized as Gaussian.
Extended Information Filter (EIF)	State distribution assumed Gaussian but parameterized by information matrix, $I = \Sigma^{-1}$ and the information vector, $\zeta = \Sigma^{-1}\mu$. Sometimes referred to as the canonical representation. Allows for processing of multiple measurements at one time easily though addition. Prediction step can be slow as it requires matrix inversion, but measurement update step is fast. Also can be time consuming to recover the mean and covariance. However, in some cases has certain advantages over the EKF.
Particle Filter (PF)	Non-parametric representation of state distribution. Instead distribution is represented by discrete particles with associated weights. Has advantage that non-Gaussian distributions and non-linear models can be incorporated. Computation scales with the number of particles in the particle set.
Least Squares Regression	Obtaining the Maximum *A Posteriori* state estimate can be formulated as a least squares optimization [7] which can be solved analytically. This formulation has the advantage that past states are maintained which can be useful for full trajectory optimization or simultaneous localization and mapping.
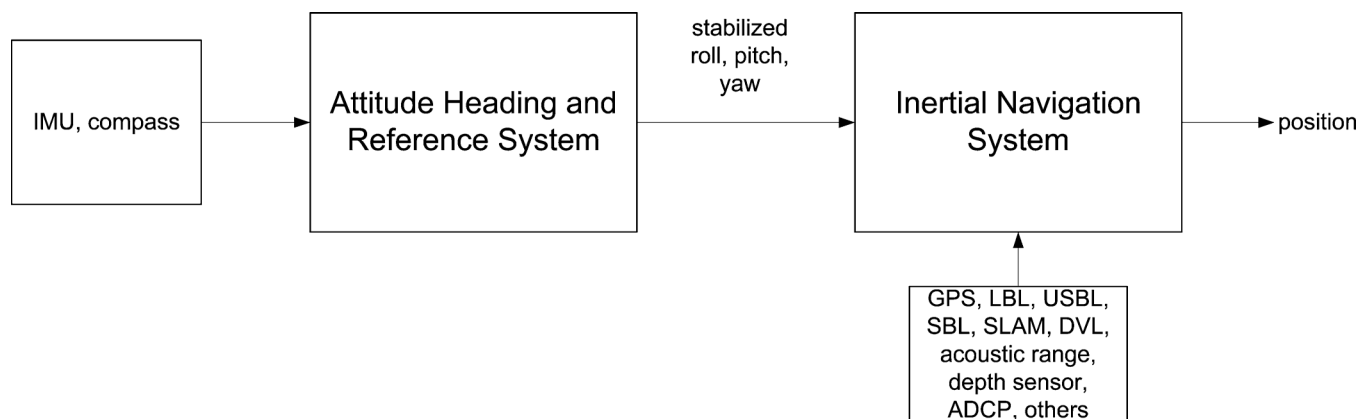
Fig. 2. Position estimation with an AHRS and an INS.

Ranges are usually projected onto the xy-plane to obtain R_{ij}^{xy} since the depths of both vehicles z_i and z_j are observable with pressure sensors

$$R_{ij}^{xy} = \left(R_{ij}^2 - (z_i - z_j)^2 \right)^{1/2}. \tag{8}$$

The range measurement model h is given by

$$h_{ij}(X_i, X_j) = \left((x_i - x_j)^2 + (y_i - y_j)^2 \right)^{1/2} + v_R \tag{9}$$

where X_i and X_j are the states of vehicles i and j with positions (x_i, y_i) and (x_j, y_j), respectively. The noise term $v_R \sim \mathcal{N}(0, \sigma_R^2)$ is zero-mean Gaussian noise. The measurement model is nonlinear and assumes that the error in the range

measurement v_R is independent of range. Some previous work has validated this assumption to some extent [58]. In [35], it is assumed that $\sigma_R = 3$ m is a reasonable value if using OWTT, and $\sigma_R = 7$ m is reasonable for RTR.

An important consideration for AUV CN, as with any CN algorithm, is to track the cross correlations that are induced from intervehicle measurements to avoid overconfidence in the estimate.

III. INERTIAL

When the AUV positions itself autonomously, with no acoustic positioning support from a ship or acoustic transponders, it dead reckons. With dead reckoning (DR), the AUV advances its position based upon knowledge of its orientation
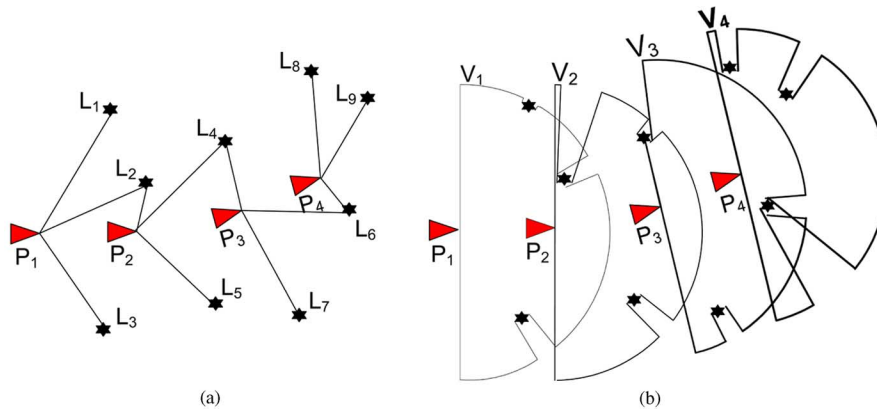
Fig. 3. (a) Feature-based SLAM, (b) View-based SLAM.

TABLE III
STRENGTHS AND WEAKNESSES OF SOME COMMON SLAM TECHNIQUES

STRENGTHS AND WEAKNESSES OF SOME COMMON SLAM TECHNIQUES

SLAM method	Pros	Cons	AUV Application
EKF SLAM [14]	Works well when features are present and distinct (which can be challenging underwater).	Adding new features to state space requires quadratic time.	[15] [16] [17] [18] [19] [20] [21] [22]
SEIF SLAM [23]	Performs updates in constant time. Due to additivity of information, it is a good choice for multiple-robot SLAM.	Information matrix has to be actively 'sparsified'. Recovering map requires matrix inversion.	[24] [25] [26]
FastSLAM [27]	Logarithmic time in number of features. No dependance on parametrization of motion models.	Ability to close loops depends on particle set.	[28] [29] [30] [31] [32]
GraphSLAM [33]	Previous poses are updated for post-processing of data.	More computation required. Covariances are hard to recover (information form).	[34] [35]
AI SLAM	Efficient, because it mimics the way animals brain work.	Requires training or parameter tuning.	[36]

and velocity or acceleration vector. Traditional DR is not considered a primary means of navigation but modern navigation systems, which depend upon DR, are widely used in AUVs. The disadvantage of DR is that errors are cumulative. Consequently, the error in the AUV position grows unbounded with distance traveled.

One simple method of DR pose estimation, for example, if heading is available from a compass and velocity is available from a Doppler velocity log (DVL), is achieved by using the following kinematic equations:

$$\dot{x} = v\cos\psi + w\sin\psi$$
$$\dot{y} = v\sin\psi + w\cos\psi$$
$$\dot{\psi} = 0 \tag{10}$$

where (x, y, ψ) is the displacement and heading in the standard north–east–down coordinate system, and v and w are the body frame forward and starboard velocities. In this model, it is assumed that roll and pitch are zero and that depth is measured accurately with a depth sensor.

An inertial system aims to improve upon the DR pose estimation by integrating measurements from accelerometers and gyroscopes. Inertial proprioceptive sensors are able to provide measurements at a much higher frequency than acoustic sensors that are based on the TOF of acoustic signals. As a result, these sensors can reduce the growth rate of pose estimation error, although it will still grow without bound.

One problem with inertial sensors is that they drift over time. One common approach, for example, used in [11], is to maintain the drift as part of the state space. Slower rate sensors are then effectively used to calibrate the inertial sensors. In [11], Miller *et al.* also track other possible sources of error such as the variable speed of sound in water to reduce systematic noise. These noise sources are propagated using a random walk model, and then updated from DVL or LBL sensor inputs. Their INS is implemented with an IMU that runs at 150 Hz.

The basic kinematics model (10) is incomplete if the local water current is not accounted for. The current can be measured with an acoustic Doppler current profiler (ADCP). For implementations with ADCP, see [9] and [10]. A DVL is usually able to calculate the velocity of the water relative to the
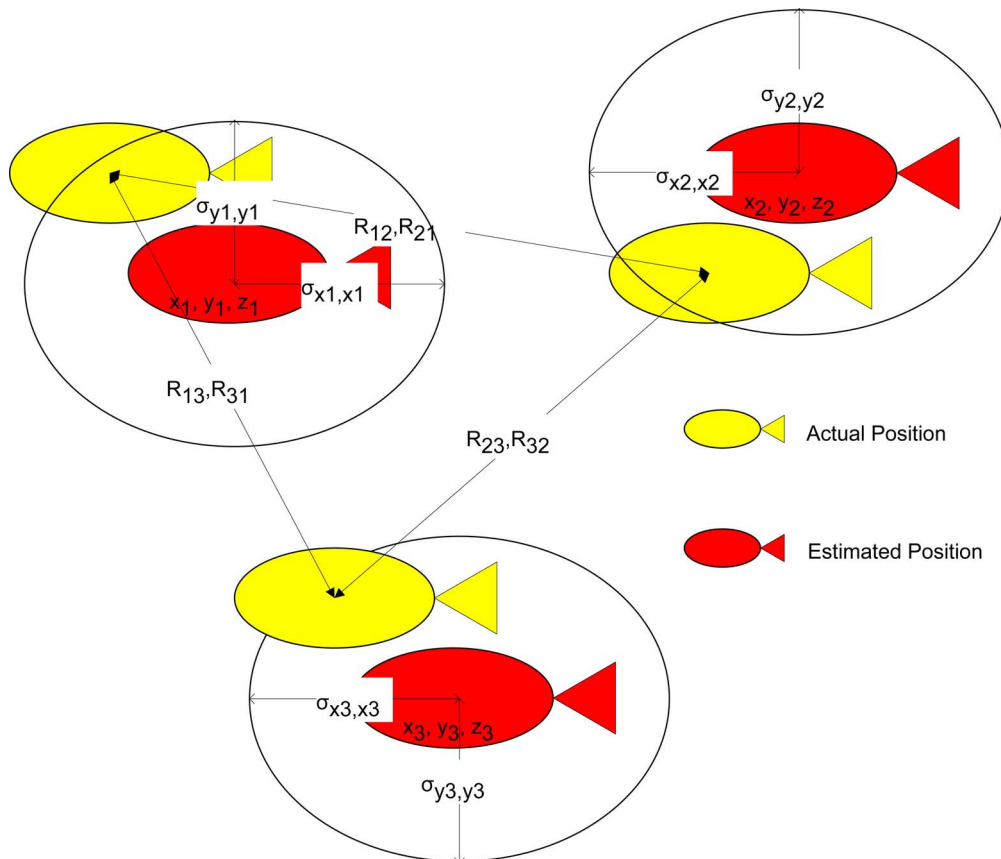
Fig. 4.   Cooperative navigation for AUVs: relative ranges are determined from TOF of acoustic communication packets.

AUV v_b and the velocity of the seabed relative to the AUV v_g. Then, the ocean current can be calculated easily as $v_c = v_g - v_b$. The ocean current can also be obtained from an ocean model, for example, in [59], where ocean currents are predicted using the regional ocean modeling system [60] combined with a Gaussian process regression [61]. If access to the velocity over the seabed is not available, then the current can be estimated from a transponder on a surface buoy as in [62]. In [62], Batista *et al.* analyzed the power spectral density to remove the low-frequency excitation on the buoy due to the waves to estimate the underwater current.

In [8], an algorithm based on particle filtering is proposed that exploits known bathymetric maps—if they exist. It is emphasized that the tide level must be carefully monitored to avoid position errors, particularly in areas of low bathymetric variation. This approach is referred to as "terrain-aided navigation," and the method is compared for DVL, and multibeam sonars as the bathymetric data input, concluding that both are viable options.

The performance of an INS is largely determined by the quality of its inertial measurement units. In general, the more expensive is the unit, the better its performance. However, the type of state estimation also has an effect. The most common filtering scheme is the EKF, but others have been used to account for the linearization and Gaussian assumption shortcomings of the EKF. For example, in [63], an unscented Kalman filter (UKF) is used, and in [64], a particle filter (PF) application is presented.

Improvements can also be made to INS navigation by modifying (10) to provide a more accurate model of the vehicle dynamics. The benefits of such an approach are investigated in [65], particularly in the case that DVL loses bottom lock, for example.

Inertial sensors are the basis of an accurate navigation scheme, and have been combined with other techniques described in Sections IV and V. In certain applications, navigation by inertial sensors is the only option. For example, in extreme depths where it is impractical to surface for Global Positioning System (GPS), an INS is used predominantly, as described in [66].

The best INS can achieve a drift of 0.1% of the distance traveled [35], however, more typical and modestly priced units can easily achieve a drift of 2%–5% of the distance traveled.

IV. ACOUSTIC TRANSPONDERS AND BEACONS

In acoustic navigation techniques, localization is achieved by measuring ranges from the TOF of acoustic signals. Common methods include the following.

- USBL: It is also sometimes called super short baseline (SSBL). The transducers on the transceiver are closely spaced with the approximated baseline on the order of less than 10 cm. Relative ranges are calculated based on the TOF and the bearing is calculated based on the difference of the phase of the signal arriving at the transceivers. See Fig. 5(b).
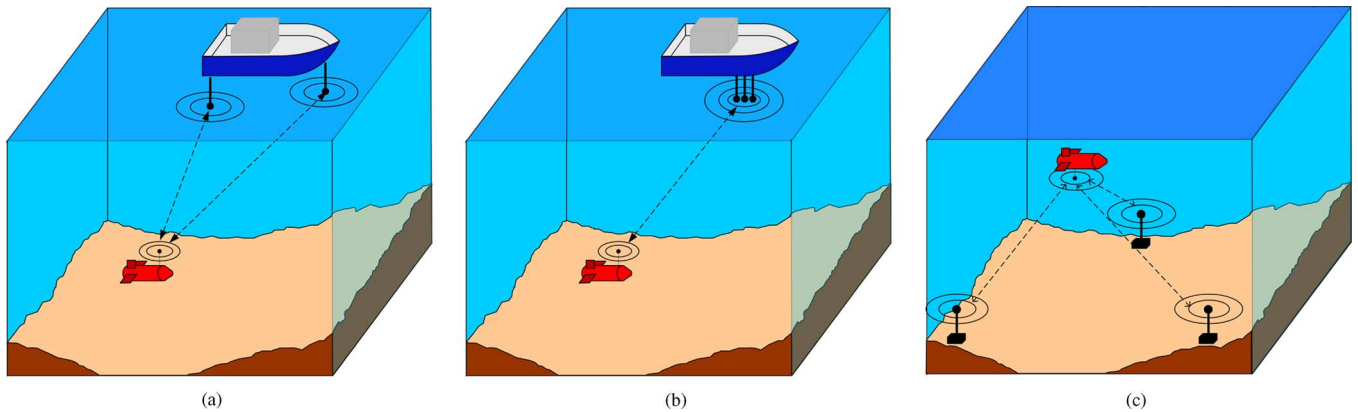
Fig. 5.   (a) SBL; (b) USBL; and (c) LBL.

- Short baseline (SBL): Beacons are placed at opposite ends of a ship's hull. The baseline is based on the size of the support ship. See Fig. 5(a).
- LBL and GPS intelligent buoys (GIBs): Beacons are placed over a wide mission area. Localization is based on triangulation of acoustic signals. See Fig. 5(c). In the case of GIBs, the beacons are at the surface, whereas for LBL they are installed on the seabed.
- Single fixed beacon: Localization is performed from only one fixed beacon.
- Acoustic modem: The recent advances with acoustic modems have allowed for new techniques to be developed. Beacons no longer have to be stationary, and full AUV autonomy can be achieved with support from autonomous surface vehicles, equipped with acoustic modems, or by communicating and ranging in underwater teams.

Due to the latency of acoustic updates, state estimators are implemented where the DR proprioceptive sensors provide the predictions and then acoustic measurements provide the updates.

A. Ultrashort and Short Baseline

USBL navigation allows an AUV to localize itself relative to a surface ship. Relative range and bearing are determined by TOF and phase differencing across an array of transceivers, respectively. A typical setup would be to have a ship supporting an AUV. In SBL, transceivers are placed at either end of the ship hull and triangulation is used.

The major limitation of USBL is the range and of SBL is that the positional accuracy is dependent on the size of the baseline, i.e., the length of the ship.

In [67], an AUV was developed to accurately map and inspect a hydro dam. A buoy equipped with a USBL and differential GPS helps to improve upon DR of the AUV which is performed using a motion reference unit (MRU), a fiber-optic gyro (FOG) and a DVL. An EKF is used to fuse the data and a mechanical scanning imaging sonar (MSIS) tracks the dam wall and follows it using another EKF. For this application, the USBL is a good choice because the range required for the mission is small. The method proposed in [12] augments [67] by using a delayed-state information filter to account for the time delay in the transmission of the surface ship position.

In [68], sensor-based integrated guidance and control is proposed using a USBL positioning system. The USBL is installed on the nose of the AUV while there is an acoustic transponder installed on a known and fixed position as a target. While homing, the USBL sensor listens for the transponder and calculates its range and bearing based on the time difference of arrival (TDOA). In [69], USBL is used for homing during the recovery of an AUV through sea ice.

In [70], two methods are presented to calibrate inertial and DVL sensors. The INS data from the AUV is sent to the surface vehicle by acoustic means. In one method, a simple KF implementation is used which maintains the inertial sensor drift errors in the state space. In the other method, possible errors of the USBL in the sound-speed profile are incorporated and the EKF is used to fuse data. No real hardware implementation is performed. In [71], the method is extended to multiple AUVs by using an "inverted" setup where the transceiver is mounted on the AUV and the transponder mounted on the surface ship.

In [72], data from an USBL and an acoustic modem are fused by a particle filter to improve DR. As a result, the vehicle operates submerged longer as GPS fixes can be less frequent. The simulation and field experiments verify the developed technique.

In [73], a "tightly coupled" approach is used where the spatial information of the acoustic array is exploited to correct the errors in the INS.

B. LBL/GPS Intelligent Buoys

In LBL navigation, localization is achieved by triangulating acoustically determined ranges from widely spaced fixed beacons. In most cases, the beacons are globally referenced before the start of the mission by a surface ship [74], a helicopter [75], or even another AUV [76]. In normal operation, an AUV would send out an interrogation signal, and the beacons would reply in a predefined sequence. The two-way travel time (TWTT) of the acoustic signals is used to determine the ranges. However, there have been implementations in which synchronized clocks are used to support OWTT ranging [77].

GIBs remove the need for the LBL beacons to be installed at the seafloor, which can reduce installation costs and the need for recovery of these beacons.

One of the limitations of LBL is the cost and time associated with setting up the network. However, this can be mitigated to

some extent if the beacon locations are not globally referenced and either self-localize [78], or the AUV can localize them by performing SLAM. For example, Newman and Leonard [34] use a nonlinear least squares implementation, whereas Petillot *et al.* [79] use a particle filter version of SLAM to determine the location of the fixed beacons during the mission.

A major consideration in an LBL localization network is the treatment of outliers. Methods to account for outliers in LBL systems include hypothesis grids [80] and graph partitioning [81]. Generally, range measurements can fall into one of three categories: direct path (DP), multipath (MP), or outlier (OL). From experience, range errors are not Gaussian distributions. The quality of range data is dependent on the location within the survey area. In [80], a hypothesis grid is built to represent the belief that future measurements from a particular cell will be in a particular category (i.e., DP, MP, and OL). In graph partitioning, outliers are rejected using spectral analysis. A set of measurements is represented as a graph, then the graph partitioning algorithm is applied to identify sets of consistent measurement [81].

Another consideration is the TDOA of the acoustic responses of the network [82], [83]. The change in vehicle pose between the initial interrogation request and all of the subsequent replies must be explicitly handled. This is often done with a delayed state EKF.

Each range difference measurement between two receivers constrains the target to an annulus (in 2-D) or a sphere (in 3-D). Annuluses are intersected to find the location of the target. However, when the data are corrupted by noise, there is not necessarily an intersection point. Sequential quadratic programming [84] is used to perform the constrained optimization. The target position estimate is the same as the traditional maximum-likelihood estimate.

Major drawbacks of LBL are the finite range imposed by the range of the beacons and the reliance on precise knowledge of the local sound-speed profile of the water column based on temperature, salinity, conductivity, and other factors [74]. However, the LBL systems do overcome these shortcomings to be one of the most robust, reliable, and accurate localization techniques available. For that reason, it is often used in high-risk situations such as under-ice surveys [75], [85]. Other implementations include: alignment of Doppler sensors [86] and deep-water surveys [87]. An extensive evaluation of the precision of LBL is provided in [88].

As a surveying implementation example, in [87], a technique is used for deep-sea near-bottom survey by an AUV which relies on LBL for navigation. LBL transponders are GPS referenced before the start of the survey.

In [86], two techniques for *in situ* three-degrees-of-freedom calibration of attitude and Doppler sonar sensors are proposed. LBL and gyrocompass measurements are sources of information for alignment.

C. Single Fixed Beacon

A downside of LBL systems is the cost and time required for installing the beacons and georeferencing them. It is possible to reduce these infrastructure requirements if only a single fixed beacon is used instead of a network of them. The concept is that
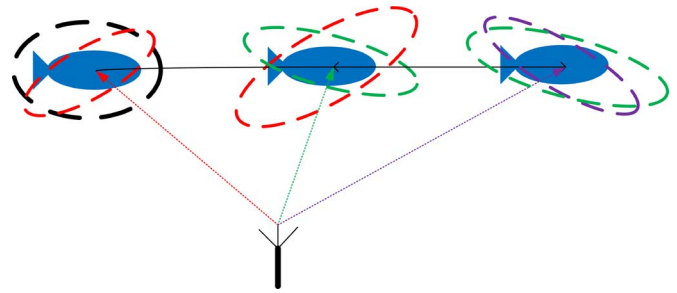

Fig. 6. An AUV localizing with a single fixed beacon at known location. Uncertainty grows in between updates from the beacon. On reception of an update from the beacon, uncertainty is reduced in the dimension coinciding with the location of the beacon.

the baseline is simulated by propagating the ranges from a single beacon forward in time until the next update is received. This technique has been referred to as virtual LBL (VLBL) and has been simulated on real-world data in [89]. It is noted that the AUV trajectory has a significant effect on the observability of the vehicle state. Long tracks directly toward or away from the single fixed beacon will cause unbounded growth in position error. As a result, tracks or paths for the survey vehicle being localized in this manner should be planned to be tangential to range circles emanating from the transponder.

A visual representation of single-beacon navigation is shown in Fig. 6. It assumes that the vehicle has prior knowledge of the beacon location. In the figure, the vehicle receives three acoustic pings from the beacon at the bottom. Each time, reception of a ping results in a reduction of uncertainty in the direction of the beacon.

An important consideration when the baseline is removed is observability of the state space. As detailed in [90], and elaborated upon in [91] and [92], if the states are estimated by a linearized filter, such as an EKF or an EIF, then observability is lost if repeated range updates come from the same relative bearing. However, if the states are estimated with a nonlinear filter, then the condition for loss of observability changes to repeated range updates coming from the same relative bearing and the same range. As a result of the nonlinear nature of the range update model, it is beneficial to use a nonlinear state estimator from an observability standpoint. This is derived in detail in [91] and [92] using Lie derivatives to generate the observability matrix.

Single-beacon navigation has also been used for homing, for example, in [93]. This task is particularly challenging because the AUV will preferentially move in a track directly toward the beacon, violating the observability criterion. As a result, path planning must be designed to avoid this situation. This can be particularly useful for recovering an AUV that has become inoperable but is still able to transmit pings.

D. Acoustic Modem

Advances in the field of acoustic communications have had a major effect on underwater navigation capabilities. The acoustic modem allows simultaneous communication of small packets and ranging based on TOF. If the position of the transmitter is included in the communicated information, then the receiver can bound its position to a sphere centered on the transmitter. This

capability removes the need for beacons to be fixed or localized prior to the mission. In addition, it allows for inter-AUV communication, which means teams of AUVs can cooperatively localize.

Popular acoustic modems are manufactured by the Woods Hole Oceanographic Institute (Woods Hole, MA, USA) [94], Teledyne Benthos (Thousand Oaks, CA, USA) [95], and EvoLogics (Berlin, Germany) [96], among others. In general, communication can either use frequency shift-keying with frequency hopping (FH–FSK), which is more reliable but provides lower data rates, or variable rate phase-coherent keying (PSK). Some models also include precise pulse-per-second (PPS) clocks (e.g., [97]) to allow synchronous ranging. Typically, due to the limited bandwidth underwater, the communication channel is shared using a TDMA scheme. In TDMA, each member in the group is allotted a time slot with which to broadcast information. The major detractor of such a scheme is that the total cycle time grows with group size. Currently, achievable bit rates range from 32 B per 10-s packet with FSK, to several kilobits per second in optimal conditions with PSK.

1) Manned Surface Support: The ability of a modem at the surface to transmit its location to the survey vehicles provides two important benefits over past navigation methods: 1) it removes the necessity to georeference the beacons before starting the mission; and 2) it allows the beacons to move during the missions. The first advantage saves time and money, and the second allows the mission range to be extended as necessary without redeploying the sensor network. Many methods have been recently published that exploit one or both of these benefits.

The moving long baseline (MLBL) concept was first demonstrated in [98] using a Sonardyne AvTrack acoustic navigation system. Two manned surface vehicles were used to support one AUV. This concept has proved particularly useful for mapping rivers, such as [99]. In this project, two boats are used to continuously define a cross section of the river to be mapped near the location of the AUV.

This approach has been extended to a single moving source. A manned surface ship can localize itself with GPS and bound the error of one or more survey AUVs by broadcasting its position. Such an approach is attractive because there is no need for calibration or recovery of beacons. The approach is similar to that presented in Section IV-C, except the mission range can be much larger because the surface vehicle can move.

In [100] and [13], a deep-water validation was performed for the single moving beacon concept. It should be noted that localization is done in postprocessing. In the proposed approach, an EKF maintains an estimate of the survey vehicle as well as the support ship. In a deep-water application, the time taken for the acoustic transmission should be accounted for in the filtering algorithm. Here, this is represented as a delayed state EKF. It is accurately noted that the TOF measured is the range between the current position of the receiver and a previous position of the sender. In [13], the performance of the single-beacon navigation is compared against an LBL system. Also, there is a more rigorous discussion on sources of error in acoustic range measurements, such as errors in sound-speed estimation, acoustic multipath, and errors in ship GPS. Similarly, in [101], a deep diving AUV is localized in postprocessing. In this case, the survey vehicle is required to execute a known closed path after it dives to a depth of 6000 m. A similar approach is presented in [102] to map the magnetic signature of a moving vessel.

If the survey vehicles are acting as passive listeners using OWTT for range measurement, then the system naturally scales well with number of survey vehicles, assuming they stay within range of the surface vehicle. In [103] and [104], a maximum-likelihood sensor fusion technique is presented to localize survey vehicles to within 1 m over a 100-km survey. It is also noted in this paper that, over a long survey, the drift of the PPS clock will have a significant effect on the localization performance.

2) Autonomous Surface Crafts: Once it is established that AUVs can navigate with the help of manned surface vehicles, a natural progression to increase autonomy is to move toward unmanned surface vehicles. The first known implementation of autonomous surface crafts (ASCs) used to support AUVs is presented in [58], which is an extension of the MLBL concept presented in [98]. Two ASCs are used to support one Odyssey III AUV in a series of experiments in 2004 and 2005. In [105], two ASCs are used and a general framework is developed for cooperative navigation.

Following previous trends, the logical progression was to perform AUV navigation and localization with only one ASC. This has been experimentally shown in [91] and [106]. The approaches taken were similar, but in [106], no actual AUVs were used in the implementation, instead an ASC was used as a surrogate. In both cases, the authors implemented a nonlinear least squares (NLSs) approach. In [91], the experimental validation is done using an ASC and an AUV to compare the performance of the EKF, PF, and an NLS optimization. It is shown that the NLS performs the best, particularly after offline postprocessing. The observability is carefully considered in both cases. In [91], it is shown that the observability criterion is less stringent if the states are being estimated with a nonlinear filter. In addition, the ASC autonomy includes basic heuristics for supporting the survey AUV and maintaining observability by performing different motion behaviors. In addition, in [91], an error analysis of the range updates is performed, and the noise is found to be relatively close to normally distributed and independent of range.

Path planning of the ASC to maintain observability is also considered explicitly in [107]. More recently, an observability analysis was done for an ASC/AUV team under the cases that position, and that position and velocity, are transmitted from the ASC to the AUV [108]. A method for globally asymptotically stable observer design is also presented. In [109], an AUV is able to localize relative to a surface ship or a drifter whose position is estimated with the use of an ocean current model. Furthermore, the AUV is able to obtain relative range and bearing estimates by detecting the surface ship or buoy using an upward-looking sonar. A theoretical analysis of the benefits of such an approach as well as performance bounds are derived.

It is expected that in the coming years, ASCs, such as the wave glider [110], will be capable of providing extremely long-term autonomous navigation capabilities. One such example scenario is presented in [111] where a wave glider is used to localize an active acoustic source.

TABLE IV
SONAR IMAGING AND RANGING DEVICES USED FOR UNDERWATER NAVIGATION

IMAGING-TYPE SONAR DEVICES USED FOR UNDERWATER NAVIGATION

Sonar	Description	Pros	Trade-Off	Application
Sidescan	multiple beams that measure intensity of returns to create a 2D image of sea bed; beams are directed perpendicular to travel direction.	can work at relatively high speeds (10kt) to give high area coverage.	resolution inversely proportional to range, e.g. 1.8 MHz produces 40 m range.	[133] [35] [134] [135]
Forward Look (imaging type)	similar in principle to a sidescan sonar only beams are directed forward.	obstacle avoidance, also as a nadir gap filler.	limited distance to depth ratio (6:1 max); single angle of view.	[26] [136]
Synthetic Aperture	coherent processing of consecutive displaced returns to synthesize a virtual array.	range independent resolution	optimal at low speeds and deeper water.	[137] [138] [139]
Mechanical Scanned Imaging Sonar	One beam with actuator that scans a swath.	Cheaper than multi-beam.	Slow. Accuracy depends on AUV attitude.	[15], [21], [140], [141], [142], [143], [22]

RANGING-TYPE SONAR DEVICES USED FOR UNDERWATER NAVIGATION

| Sonar	Description	Pros	Trade-Off	Application
Echo Sounder	single, narrow beam used to determine depth below the transducer.	yield representation of sea bed and targets between transducer to seabed.	point measurements in generally one direction.	[144], [145]
Profiler	low-frequency echo sounders that penetrate the seabed.	information on subsurface features.	penetration depth inversely proportional to resolution.	[146]
Multi-Beam	time-of-flight from returns to assemble bathymetric maps.	gathers echo sounding data more efficiently than a single beam.	resolution inversely proportional to frequency; may not always capture the first ping.	[28] [29] [30] [31]
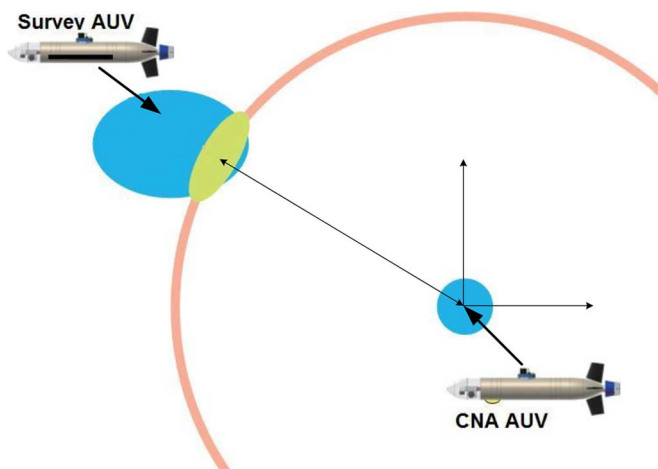
Fig. 7. A CNA AUV supporting a survey AUV [112]. The blue areas are the vehicle uncertainty ellipses. The yellow area is the updated uncertainty of the survey ellipse from a range measurement, which is shown in pink.

3) Heterogeneous AUV Teams: In some cases, certain AUVs are outfitted with more expensive sensors and/or make frequent trips to surface for GPS position fixes. These vehicles support the other survey vehicles and have been referred to as communication/navigation aids (CNAs).[2] An application would be to have inferior navigation sensors on a fleet of survey vehicles and expensive navigation sensors on only a small number of vehicles whose job is to support that fleet [112]. Upon reception of a CNA transmission the receiver's position estimate can be restricted to an annulus if each vehicle has a good estimate of depth (which can easily be obtained from a pressure sensor), and if the receiver can estimate its range to the CNA, for example, through either one-way TOF of the acoustic signal (requires synchronized clocks) or two-way TOF. This annulus can be intersected with a vehicle's own covariance ellipse, as shown in Fig. 7.

The framework for cooperative navigation developed by Bahr *et al.* is presented in [113], [105], [114], and [115] and is applicable to general AUV teams. Referring to Fig. 7, each annulus is propagated forward in time until the next update is received from the CNA. In between updates, the uncertainty grows based on the quality of the DR estimation. The importance of careful bookkeeping and maintenance of cross correlations between survey and CNA AUVs is stressed to

[2]This term has also been applied to surface vehicles supporting AUV survey teams.

avoid overconfidence and to enhance the quality of outlier rejection. While the developed framework is to be used for pure AUV systems, all results show the use of ASCs as "surrogate AUVs."

An altogether different approach to CN is presented in [116] where a hovering type AUV can physically dock to the torpedo-type AUV to exchange information.

4) Homogeneous AUV Teams: When a homogeneous team performs CN, each member of the team is treated equally. Position error will grow slower if the AUVs are able to communicate their relative positions and ranges. Similarly to the heterogeneous case, if any vehicle surfaces for a position fix, then the information can be shared with the rest of the team to bound the position error.

The first known experimental implementation of such a system was in 2007 [117]. In this approach, the vehicle states are maintained with an EKF but cross covariances are not transmitted in the communication packet due to bandwidth limitations. The communication latency is accounted for in the EKF implementation.

More recently, an implementation of CN was presented in [118]. Here, the issue of bookkeeping is explicitly addressed. A multivehicle ledger system is used so updates are only made to the multivehicle EKF when all up to date data have been obtained. Experiments were performed with kayaks acting as AUV surrogates, where OWTT ranging was done with the synchronized clocks in a 30-s cycle, each of the three vehicles having a 10-s slot to make a transmission.

V. Geophysical

Geophysical navigation refers to any method that utilizes external environmental features for localization. Almost all methods in this category that achieve the bounded position error use some form of SLAM. Categories include the following.

- Magnetic: It has been proposed to use magnetic field maps for localization. Although no recent publications have been found, a team at the University of Idaho (Moscow, ID, USA) has been mapping the magnetic signatures of Navy vessels [119], [120].
- Optical: Use of a monocular or stereo camera to capture images of the seabed and then match these images to navigate.
- Sonar: Used to acoustically detect then identify and classify features in the environment that could be used as navigation landmarks. With bathymetric sonar, features can be extracted almost directly from assembled returns. With sidescan (imaging) sonar, feature extraction is achieved through processing of imagery.

A. Optical

Visual odometry is the process of determining the robot pose by analyzing subsequent camera images. This can be achieved through optical flow or structure from motion (SFM). Invariant extraction and representation of features is an important consideration. Many previous algorithms have been proposed and applied in ground and air robotics, such as scale-invariant feature transform (SIFT) [121], speeded up robust feature (SURF)

[122], among many others.[3] Images can be captured with either stereo or monocular cameras. Stereo cameras have the added advantage that full six degree-of-freedom transformations between consecutive image pairs can be found. Vision-based SLAM can also be performed with the methods presented in Table III. The major challenge is closing loops in the trajectory by associating nonconsecutive images, which is necessary to bound the localization error.

Limitations for optical systems in underwater environments include the reduced range of cameras, susceptibility to scattering, and inadequacy of lighting. As a result, visible wavelength cameras are more commonly installed on hovering AUVs because they can get close to objects of interest. In addition, visual odometry and feature extraction relies on the existence of features. Therefore, optical underwater navigation methods are particularly well suited to small-scale mapping of feature-rich environments. Examples include ship hulls or shipwreck inspections.

In [16] and [17], Eustice *et al.* present an implementation of underwater vision-based SLAM, called visually augmented navigation (VAN). The multisensor approach combines the benefits of optical and inertial navigation methods and is robust to low overlap of imagery. The approach is a view-based version of EKF–SLAM, where camera-derived relative pose measurements provide the spatial constraints for visual odometry and loop closure. In [24] and [25], the VAN approach is converted to the information form, and it is proven that the view-based ESEIF–SLAM maintains a sparse information matrix without approximations or pruning. This approach was applied to deepwater surveying of the *RMS Titanic* in [24]. The issue of recovering the mean and the covariance from the information form is also addressed. SIFT and Harris extraction points are used to match images. The VAN method has also been applied to ship-hull inspection for the U.S. Navy [124]. Both [44] and [125] were inspired by the VAN method. However, these two methods improved upon the approach using a smoothing and mapping problem formulation and doing efficient matrix factorizations to be able to efficiently recover the means and covariances. In recent work, Hover *et al.* [126] use features from both a profiling sonar and a monocular camera in full pose graph formulation for a hovering AUV performing ship-hull inspections. Odometry is derived relative to the ship hull using a DVL locked onto the ship. An approach to tackle the problem of data association in feature-poor areas of a ship hull is explored in [127], using a novel online bag-of-words approach to determine interimage and intraimage saliency.

Feature-based approaches to underwater SLAM have also been done. For example, in [18], an augmented EKF is used to generate a topological representation. Non-time-consecutive images are compared and loop closures are made based on observation mutual information. Feature-based EKF–SLAM is also applied to the underwater environment in [19] and [20].

A byproduct of accurate localization is that accurate mapping can be achieved. Several authors have shown the ability to compute 2-D and 3-D reconstructions of the underwater environment based on optical underwater SLAM. For example,

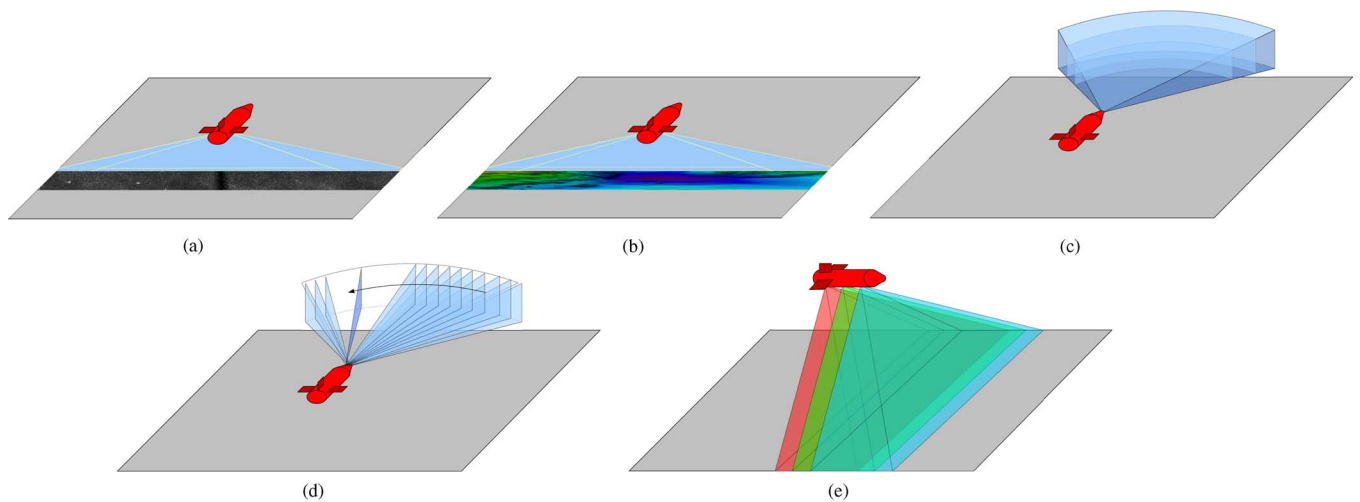[3]For a review and comparison of some methods, see [123].

Fig. 8.   Sonar sensor swaths: (a) sidescan, (b) multibeam, (c) forward looking, (d) mechanical scanning and imaging, and (e) synthetic aperture.

in [128], an SFM model together with SLAM is used to photomosaic the *RMS Titanic* as well as a hydrothermal vent area in the mid-Atlantic. In [129], 3-D reconstructions of an underwater environment are done using SLAM with a combination of multibeam sonar and stereo camera.

Future research will likely involve incorporating multiple vehicles. Recently, some publications involving simulations reported on this [130], [131]. Overcoming communication constraints will be a major challenge.

Pure visual odometry-based methods that do not require SLAM can be used for applications such as pipeline tracking [132].

B. Sonar

Sonar imaging of the ocean predates AUVs by decades. As a result, it is a fairly robust technology. Several types of sonars are used for seabed and structure mapping. They are summarized in Table IV.

Sonars are designed to operate at specific frequencies [147] depending on the range and resolution required. In all cases, the performance of the SLAM algorithm is dependent on the number and quality of the features present in the environment.

1) Imaging Sonar: The insonified swath of the sidescan sonar is shown in Fig. 8(a). The intensity of the acoustic returns from the seabed of this fan-shaped beam also depends on the bottom type and is recorded in a series of cross-track slices. When mosaicked together along the direction of travel, these assembled slices form an image of the seabed within the swath of the beam. Hard objects protruding from the seabed send a strong return which is represented as a dark image. Shadows and soft areas, such as mud and sand, send weaker returns which are represented as lighter images.

SLAM with the sidescan was first presented in [133] using an augmented EKF and the Rauch–Tung–Striebel smoother. The value of smoothing in the pose estimation is emphasized since all previous poses should be updated when a loop closure event is detected. It is noted that automated feature detection (which is not trivial) and data association are necessary to achieve autonomy for sidescan sonar SLAM. In [35], the approach in

[133] is improved using iSAM for smoothing and incorporates range updates from a CNA. This is the only known research that combines a sonar-based SLAM method with acoustic modem ranging. In [134], sidescan sonar SLAM is posed as an interval constraint propagation problem. In [148] and [135], the problem was approached using a submap joining algorithm called the selective submap joining SLAM. The work in [135] uses a cascaded Haar classifier for object detection from sidescan imagery and is demonstrated offline on a gathered data set. A discussion of which type of features is appropriate for sidescan sonar SLAM is presented in [149]. All of the proposed approaches to sidescan sonar SLAM require postprocessing to detect the features for data association. Presently, this is just becoming achievable onboard AUVs.

A depiction of the forward-looking sonar (FLS) is shown in Fig. 8(c). Based on the transducer geometry, the primary function of this type of sonar device is to map vertical features. As such it is commonly deployed on a hovering AUV capable of approaching man-made underwater structures at very low speeds. Feature-based SLAM based on ESEIF has also been implemented with an FLS for ship-hull inspections [26]. The issue of online feature extraction from FLS images is addressed in [136].

The mechanical scanning imaging sonar (MSIS) is shown in Fig. 8(d). Its operation is similar to the FLS except that, instead of multiple beams, a single beam is rotated through the desired viewing angle. Consequently, the update rate is slow. It cannot be assumed that the AUV pose is constant for an entire sensor scan cycle, which increases the complexity of mapping algorithms.

A group at the University of Girona (Girona, Spain) has done significant work with the MSIS, as presented in [15], [21], [140]–[143], and [22]. In [15] and [22], online feature extraction and data association and an EKF–SLAM implementation were performed. In addition, a submap method was used to reduce computational complexity. Given that the algorithm is based on line feature extraction, the method is well suited to man-made environments with well-defined edges and boundaries. In [21], the slow update rate of the MSIS was accounted

for with a delayed state EKF–SLAM algorithm. In [142], [141], [140], and [143], a probabilistic scan matching algorithm was presented that exploited the overlap in the images from the MSIS.

A figure depicting the synthetic aperture sonar (SAS) is shown in Fig. 8(e). Synthetic aperture is a methodology that enables high resolution through coherent processing of consecutive displaced returns. Instead of using a large static array of transducers, it uses the sensor's along-track displacement to create a large virtual array. The resulting resolution is on the order of the transducer dimensions and, more importantly, independent of the range between the sensor and the target. Since there is no need to have a small aperture the frequency used can be considerably lower, which enables a longer range since lower frequencies propagate further in water. This is at the cost of more complex image processing and the requirement for a tightly prescribed speed. The micronavigation required to attain the tightly prescribed speed and trajectory, in the presence of seas, is an active area of research.

Applications of SAS to AUV navigation represent an area of active investigation. Both [137] and [138] describe a displaced phase center antenna micronavigation technique using SAS, which is good at estimating sway, but poor at estimating yaw. In [139], a constant time SLAM algorithm was developed for use with a SAS. The approach uses a submap approach to maintain scalability. Data association is done offline and comparisons with ground truth provided by LBL show good results. An additional comment about SAS for navigation is that, although it offers remarkable detection capabilities, the SAS payload can significantly change the hydrodynamics and controllability of a small AUV [139].

2) Ranging Sonar: A depiction of the multibeam sensor swath is shown in Fig. 8(b). With multibeam instead of just one transducer pointing down there are multiple beams from arrays of transducers arranged in a precise pattern on an AUV hull. The sound bounces off the seafloor at different angles and is received by the AUV at slightly different times. The signals are then processed onboard the AUV, converted into water depths, and arranged as a bathymetric map. The multibeam resolution achieved depends on its transducer quality, operating frequency, and altitude from the seabed. Multibeam bathymetry systems have been routinely used to map out large areas of seafloor. Each survey line that the AUV transits collects a corridor of data known as a swath. The multibeam sonar yields 2.5-D bathymetric features (elevation map) whereas the sidescan sonar produces 2-D imagery. The former better facilitates feature-based navigation, as evidenced in the literature [28], [29].

Barkby *et al.* have proposed a bathymetric SLAM algorithm called BPSLAM that is based on a featureless FastSLAM implementation [28]–[31]. In their approach, the need for feature extraction is removed; each particle maintains an estimate of the current vehicle state and the 2-D bathymetric map. An important issue with employing a particle-filter-based system with such a large state space is the computational expense of copying particles' maps during the resampling process. This problem is solved by "distributed particle mapping" where a particle ancestry tree is maintained. Copying of particle maps is avoided by having new particles generated during the resampling process point to their parents' maps rather than copying them. Maps of leaf nodes in the tree are reconstructed by recombining the maps of all ancestors. In [28], the need to store each particle's map is removed completely by storing just the particle's trajectory and linking poses to an entry in a log of bathymetry observations. Maps are then reconstructed as needed using Gaussian process regression, and, as a result, loop closures can be achieved even in the case where there is little or no overlap between sonar images since the regression process is able to make predictions about areas of seabed that have not been directly observed.

Similar to optical SLAM, the higher is the quality of the navigation algorithm, the higher the quality of the data. A convenient way of representing 3-D data is in octree form as in [32]. In this work, an active localization framework is presented where actions are selected to reduce the entropy of particles. The vehicle pose is estimated with particle filter SLAM.

Using phase-only matched filtering for comparing subsequent images is presented in [150] and later [151]. It is shown that this method outperforms the standard iterative closest point method to find six degree-of-freedom transformations between subsequent multibeam scans. A similar approach using planar surface registration is presented in [152].

VI. Conclusion

A review of recent advances in underwater localization and navigation has been performed. In addition, some basic methods of state estimation and SLAM have been presented. The algorithms are subdivided based on the technical approach, sensors used, and level of collaboration, as shown in Fig. 1. We have also highlighted some areas for future work in the field.

Recent advances in acoustic communications and SLAM have allowed for rapid development of new underwater localization algorithms. The acoustic modem is realizing the possibility of underwater collaboration, and sonar and optical sensors performing SLAM can achieve bounded localization. While some of these methods are still not well formalized or tested, it is clear that the limitations of legacy systems such as LBL, USBL, and others can be overcome with these new techniques.

The harsh and unstructured nature of the underwater environment causes significant challenges for underwater autonomous systems. However, with recent advances, this field is progressing at an unprecedented rate.

References

[1] L. Stutters, H. Liu, C. Tiltman, and D. Brown, "Navigation technologies for autonomous underwater vehicles," *IEEE Trans. Syst. Man Cybern. C, Appl. Rev.*, vol. 38, no. 4, pp. 581–589, Jul. 2008.

[2] J. J. Leonard, A. A. Bennett, C. M. Smith, and H. J. S. Feder, "Autonomous underwater vehicle navigation," MIT Marine Robot. Lab., Cambridge, MA, USA, Tech. Memo., 1998.

[3] J. C. Kinsey, R. M. Eustice, and L. L. Whitcomb, "A survey of underwater vehicle navigation: Recent advances and new challenges," in *Proc. Conf. Manoeuvering Control Marine Craft*, 2006, pp. 1–12.

[4] Klein Associates, Salem, NH, USA [Online]. Available: http://www.l-3klein.com

[5] M. De Agostino, A. Manzino, and M. Piras, "Performances comparison of different MEMS-based IMUs," in *Proc. IEEE/ION Position Locat. Navig. Symp.*, 2010, pp. 187–201.

[6] S. Thrun, W. Burgard, and D. Fox, *Probabilistic Robotics*. Cambridge, MA, USA: MIT Press, 2005, pp. 13–437.

[7] D. Frank and K. Michael, "Square root SAM: Simultaneous location and mapping via square root information smoothing," *Int. J. Robot. Res.*, vol. 25, no. 12, pp. 1181–1203, 2006.

[8] G. Donovan, "Position error correction for an autonomous underwater vehicle inertial navigation system (INS) using a particle filter," *IEEE J. Ocean. Eng.*, vol. 37, no. 3, pp. 431–445, Jul. 2012.

[9] B. Garau, A. Alvarez, and G. Oliver, "AUV navigation through turbulent ocean environments supported by onboard H-ADCP," in *Proc. IEEE Int. Conf. Robot. Autom.*, May 2006, pp. 3556–3561.

[10] O. Hegrenaes and E. Berglund, "Doppler water-track aided inertial navigation for autonomous underwater vehicle," in *Proc. OCEANS Eur. Conf.*, May 2009, DOI: 10.1109/OCEANSE.2009.5278307.

[11] P. Miller, J. Farrell, Y. Zhao, and V. Djapic, "Autonomous underwater vehicle navigation," *IEEE J. Ocean. Eng.*, vol. 35, no. 3, pp. 663–678, Jul. 2010.

[12] D. Ribas, P. Ridao, A. Mallios, and N. Palomeras, "Delayed state information filter for USBL-aided AUV navigation," in *Proc. IEEE Int. Conf. Robot. Autom.*, May 2012, pp. 4898–4903.

[13] S. E. Webster, R. M. Eustice, H. Singh, and L. L. Whitcomb, "Advances in single-beacon one-way-travel-time acoustic navigation for underwater vehicles," *Int. J. Robot.*, vol. 31, no. 8, pp. 935–950, 2012.

[14] R. C. Smith and P. Cheeseman, "On the representation and estimation of spatial uncertainty," *Int. J. Robot. Res.*, vol. 5, no. 4, pp. 56–68, 1986.

[15] D. Ribas, P. Ridao, J. D. Tardós, and J. Neira, "Underwater SLAM in man-made structured environments," *J. Field Robot.*, vol. 25, no. 11–12, pp. 898–921, 2008.

[16] R. Eustice, "Large-area visually augmented navigation for autonomous underwater vehicles," Ph.D. dissertation, Massachusetts Inst. Technol./Woods Hole Oceanogr. Inst., Cambridge/Woods Hole, MA, USA, 2005.

[17] R. Eustice, O. Pizarro, and H. Singh, "Visually augmented navigation for autonomous underwater vehicles," *IEEE J. Ocean. Eng.*, vol. 33, no. 2, pp. 103–122, Apr. 2008.

[18] A. Elibol, N. Gracias, and R. Garcia, "Augmented state extended Kalman filter combined framework for topology estimation in large-area underwater mapping," *J. Field Robot.*, vol. 27, no. 5, pp. 656–674, 2010.

[19] J. Salvi, Y. Petillot, and E. Batlle, "Visual SLAM for 3D large-scale seabed acquisition employing underwater vehicles," in *Proc. IEEE/RSJ Int. Conf. Intell. Robots Syst.*, Sep. 2008, pp. 1011–1016.

[20] J. Salvi, Y. Petillot, S. Thomas, and J. Aulinas, "Visual SLAM for underwater vehicles using video velocity log and natural landmarks," in *Proc. OCEANS Conf.*, Sep. 2008, DOI: 10.1109/OCEANS.2008.5151887.

[21] D. Ribas, P. Ridao, J. Neira, and J. Tardos, "SLAM using an imaging sonar for partially structured underwater environments," in *Proc. IEEE/RSJ Int. Conf. Intell. Robots Syst.*, Oct. 2006, pp. 5040–5045.

[22] D. Ribas, P. Ridao, J. Tardos, and J. Neira, "Underwater SLAM in a marina environment," in *Proc. IEEE/RSJ Int. Conf. Intell. Robots Syst.*, Nov. 2007, pp. 1455–1460.

[23] S. Thrun, Y. Liu, D. Koller, A. Y. Ng, Z. Ghahramani, and H. Durrant-Whyte, "Simultaneous localization and mapping with sparse extended information filters," *Int. J. Robot. Res.*, vol. 23, no. 7–8, pp. 693–716, 2004.

[24] R. M. Eustice, H. Singh, J. J. Leonard, and M. R. Walter, "Visually mapping the RMS Titanic: Conservative covariance estimates for SLAM information filters," *Int. J. Robot. Res.*, vol. 25, no. 12, pp. 1223–1242, 2006.

[25] R. Eustice, H. Singh, and J. Leonard, "Exactly sparse delayed-state filters for view-based SLAM," *IEEE Trans. Robot.*, vol. 22, no. 6, pp. 1100–1114, Dec. 2006.

[26] M. Walter, F. Hover, and J. Leonard, "SLAM for ship hull inspection using exactly sparse extended information filters," in *Proc. IEEE Int. Conf. Robot. Autom.*, May 2008, pp. 1463–1470.

[27] M. Montemerlo, S. Thrun, D. Koller, and B. Wegbreit, "FastSLAM: A factored solution to the simultaneous localization and mapping problem," in *Proc. AAAI Nat. Conf. Artif. Intell.*, 2002, pp. 593–598.

[28] S. Barkby, S. B. Williams, O. Pizarro, and M. V. Jakuba, "Bathymetric particle filter SLAM using trajectory maps," *Int. J. Robot. Res.*, vol. 31, no. 12, pp. 1409–1430, 2012.

[29] S. Barkby, S. B. Williams, O. Pizarro, and M. V. Jakuba, "A featureless approach to efficient bathymetric SLAM using distributed particle mapping," *J. Field Robot.*, vol. 28, no. 1, pp. 19–39, 2011.

[30] S. Barkby, S. Williams, O. Pizarro, and M. Jakuba, "Incorporating prior maps with bathymetric distributed particle SLAM for improved AUV navigation and mapping," in *Proc. MTS/IEEE OCEANS Conf.*, Oct. 2009, pp. 1–7.

[31] S. Barkby, S. Williams, O. Pizarro, and M. Jakuba, "An efficient approach to bathymetric SLAM," in *Proc. IEEE/RSJ Int. Conf. Intell. Robots Syst.*, Oct. 2009, pp. 219–224.

[32] N. Fairfield and D. Wettergreen, "Active localization on the ocean floor with multibeam sonar," in *Proc. OCEANS Conf.*, Sept. 2008, DOI: 10.1109/OCEANS.2008.5151853.

[33] F. Lu and E. Milios, "Globally consistent range scan alignment for environment mapping," *Autonom. Robots*, vol. 4, pp. 333–349, 1997.

[34] P. Newman and J. Leonard, "Pure range-only sub-sea SLAM," in *Proc. IEEE Int. Conf. Robot. Autom.*, Sep. 2003, vol. 2, pp. 1921–1926.

[35] M. F. Fallon, M. Kaess, H. Johannsson, and J. J. Leonard, "Efficient AUV navigation fusing acoustic ranging and side-scan sonar," in *Proc. IEEE Int. Conf. Robot. Autom.*, May 2011, pp. 2398–2405.

[36] B. Howell and S. Wood, "Passive sonar recognition and analysis using hybrid neural networks," in *Proc. OCEANS Conf.*, 2003, vol. 4, pp. 1917–1924.

[37] M. Bosse and R. Zlot, "Map matching and data association for large-scale two-dimensional laser scan-based SLAM," *Int. J. Robot. Res.*, vol. 27, no. 6, pp. 667–691, 2008.

[38] H. Durrant-Whyte and T. Bailey, "Simultaneous localization and mapping (SLAM): Part I the essential algorithms," *IEEE Robot. Autom. Mag.*, vol. 13, no. 3, pp. 108–117, 2006.

[39] M. R. Walter, R. M. Eustice, and J. J. Leonard, "Exactly sparse extended information filters for feature-based SLAM," *Int. J. Robot. Res.*, vol. 26, no. 4, pp. 335–359, 2007.

[40] G. Grisetti, C. Stachniss, and W. Burgard, "Improved techniques for grid mapping with Rao-Blackwellized particle filters," *IEEE Trans. Robot.*, vol. 23, no. 1, pp. 34–46, Feb. 2007.

[41] A. Howard, M. Mataric, and G. Sukhatme, "Relaxation on a mesh: A formalism for generalized localization," in *Proc. IEEE/RSJ Int. Conf. Intell. Robots Syst.*, 2001, vol. 2, pp. 1055–1060.

[42] U. Frese, P. Larsson, and T. Duckett, "A multilevel relaxation algorithm for simultaneous localization and mapping," *IEEE Trans. Robot.*, vol. 21, no. 2, pp. 196–207, Apr. 2005.

[43] E. Olson, J. Leonard, and S. Teller, "Fast iterative alignment of pose graphs with poor initial estimates," in *Proc. IEEE Int. Conf. Robot. Autom.*, 2006, pp. 2262–2269.

[44] M. Kaess, A. Ranganathan, and F. Dellaert, "iSAM: Incremental smoothing and mapping," *IEEE Trans. Robot.*, vol. 24, no. 6, pp. 1365–1378, Dec. 2008.

[45] G. Grisetti, C. Stachniss, and W. Burgard, "Nonlinear constraint network optimization for efficient map learning," *IEEE Trans. Intell. Transp. Syst.*, vol. 10, no. 3, pp. 428–439, Sep. 2009.

[46] G. Grisetti, R. Kümmerle, C. Stachniss, and W. Burgard, "A tutorial on graph-based SLAM," *IEEE Intell. Transp. Syst. Mag.*, vol. 2, no. 4, pp. 31–43, Winter, 2010.

[47] G. Grisetti, R. Kümmerle, C. Stachniss, U. Frese, and C. Hertzberg, "Hierarchical optimization on manifolds for online 2D and 3D mapping," in *Proc. IEEE Int. Conf. Robot. Autom.*, 2010, pp. 273–278.

[48] G. Wyeth and M. Milford, "Spatial cognition for robots," *IEEE Robot. Autom. Mag.*, vol. 16, no. 3, pp. 24–32, Sep. 2009.

[49] S. Saeedi, L. Paull, M. Trentini, and H. Li, "Neural network-based multiple robot simultaneous localization and mapping," *IEEE Trans. Neural Netw.*, vol. 22, no. 12, pp. 2376–2387, Dec. 2011.

[50] S. Roumeliotis and G. Bekey, "Distributed multirobot localization," *IEEE Trans. Robot. Autom.*, vol. 18, no. 5, pp. 781–795, Oct. 2002.

[51] S. I. Roumeliotis and I. M. Rekleitis, "Propagation of uncertainty in cooperative multirobot localization: Analysis and experimental results," *Autonom. Robots*, vol. 17, pp. 41–54, 2004.

[52] A. Mourikis and S. Roumeliotis, "Performance analysis of multirobot cooperative localization," *IEEE Trans. Robot.*, vol. 22, no. 4, pp. 666–681, Aug. 2006.

[53] E. Nerurkar, S. Roumeliotis, and A. Martinelli, "Distributed maximum a posteriori estimation for multi-robot cooperative localization," in *Proc. IEEE Int. Conf. Robot. Autom.*, May 2009, pp. 1402–1409.

[54] N. Trawny, S. Roumeliotis, and G. Giannakis, "Cooperative multi-robot localization under communication constraints," in *Proc. IEEE Int. Conf. Robot. Autom.*, May 2009, pp. 4394–4400.

[55] G. Huang, N. Trawny, A. Mourikis, and S. Roumeliotis, "Observability-based consistent EKF estimators for multi-robot cooperative localization," *Autonom. Robots*, vol. 30, pp. 99–122, 2011.

[56] X. Zhou and S. Roumeliotis, "Robot-to-robot relative pose estimation from range measurements," *IEEE Trans. Robot.*, vol. 24, no. 6, pp. 1379–1393, Dec. 2008.

[57] Y. Dieudonne, O. Labbani-Igbida, and F. Petit, "Deterministic robot-network localization is hard," *IEEE Trans. Robot.*, vol. 26, no. 2, pp. 331–339, Apr. 2010.

[58] J. Curcio, J. Leonard, J. Vaganay, A. Patrikalakis, A. Bahr, D. Battle, H. Schmidt, and M. Grund, "Experiments in moving baseline navigation using autonomous surface craft," in *Proc. MTS/IEEE OCEANS Conf.*, 2005, pp. 730–735.

[59] G. A. Hollinger, A. A. Pereira, V. Ortenzi, and G. S. Sukhatme, "Towards improved prediction of ocean processes using statistical machine learning," in *Proc. Robotics, Sci. Syst. Workshop Robot. Environ. Monitoring*, Sydney, Australia, Jul. 2012 [Online]. Available: http://robotics.usc.edu/publications/775/

[60] A. F. Shchepetkin and J. C. McWilliams, "The regional oceanic modeling system (ROMS): A split-explicit, free-surface, topography-following-coordinate oceanic model," *Ocean Model.*, vol. 9, no. 4, pp. 347–404, 2005.

[61] C. E. Rasmussen, *Gaussian Processes for Machine Learning*. Cambridge, MA, USA: MIT Press, 2006, pp. 26–51.

[62] P. T. M. Batista, C. Silvestre, and P. J. R. Oliveira, "Optimal position and velocity navigation filters for autonomous vehicles," *Automatica*, vol. 46, no. 4, pp. 767–774, 2010.

[63] G. Karras, S. Loizou, and K. Kyriakopoulos, "On-line state and parameter estimation of an under-actuated underwater vehicle using a modified dual unscented Kalman filter," in *Proc. IEEE/RSJ Int. Conf. Intell. Robots Syst.*, Oct. 2010, pp. 4868–4873.

[64] L. Huang, B. He, and T. Zhang, "An autonomous navigation algorithm for underwater vehicles based on inertial measurement units and sonar," in *Proc. 2nd Int. Asia Conf. Inf. Control Autom. Robot.*, Mar. 2010, vol. 1, pp. 311–314.

[65] O. Hegrenaes and O. Hallingstad, "Model-aided INS with sea current estimation for robust underwater navigation," *IEEE J. Ocean. Eng.*, vol. 36, no. 2, pp. 316–337, Apr. 2011.

[66] L. Whitcomb, M. Jakuba, J. Kinsey, S. Martin, S. Webster, J. Howland, C. Taylor, D. Gomez-Ibanez, and D. Yoerger, "Navigation and control of the Nereus hybrid underwater vehicle for global ocean science to 10,903 m depth: Preliminary results," in *Proc. IEEE Int. Conf. Robot. Autom.*, May 2010, pp. 594–600.

[67] P. Ridao, M. Carreras, D. Ribas, and R. Garcia, "Visual inspection of hydroelectric dams using an autonomous underwater vehicle," *J. Field Robot.*, vol. 27, no. 6, pp. 759–778, 2010.

[68] P. Batista, C. Silvestre, and P. Oliveira, "A sensor-based controller for homing of underactuated AUVs," *IEEE Trans. Robot.*, vol. 25, no. 3, pp. 701–716, Jun. 2009.

[69] A. Plueddemann, A. Kukulya, R. Stokey, and L. Freitag, "Autonomous underwater vehicle operations beneath coastal sea ice," *IEEE/ASME Trans. Mechatron.*, vol. 17, no. 1, pp. 54–64, Feb. 2012.

[70] Y. Watanabe, H. Ochi, T. Shimura, and T. Hattori, "A tracking of AUV with integration of SSBL acoustic positioning and transmitted INS data," in *Proc. OCEANS Eur. Conf.*, May 2009, DOI: 10.1109/OCEANSE.2009.5278145.

[71] Y. Watanabe, H. Ochi, and T. Shimura, "A study of inverse SSBL acoustic positioning with data transmission for multiple AUV navigation," in *Proc. OCEANS Conf.*, May 2012, DOI: 10.1109/OCEANS-Yeosu.2012.6263632.

[72] R. Khan, T. Taher, and F. Hover, "Accurate geo-referencing method for AUVs for oceanographic sampling," in *Proc. OCEANS Conf.*, Sep. 2010, DOI: 10.1109/OCEANS.2010.5664570.

[73] M. Morgado, P. Oliveira, and C. Silvestre, "Tightly coupled ultrashort baseline and inertial navigation system for underwater vehicles: An experimental validation," *J. Field Robot.*, vol. 30, no. 1, pp. 142–170, 2013.

[74] N. Kussat, C. Chadwell, and R. Zimmerman, "Absolute positioning of an autonomous underwater vehicle using GPS and acoustic measurements," *IEEE J. Ocean. Eng.*, vol. 30, no. 1, pp. 153–164, Jan. 2005.

[75] M. V. Jakuba, C. N. Roman, H. Singh, C. Murphy, C. Kunz, C. Willis, T. Sato, and R. A. Sohn, "Long-baseline acoustic navigation for under-ice autonomous underwater vehicle operations," *J. Field Robot.*, vol. 25, no. 11–12, pp. 861–879, 2008.

[76] I. Vasilescu, C. Detweiler, M. Doniec, D. Gurdan, S. Sosnowski, J. Stumpf, and D. Rus, "AMOUR V: A hovering energy efficient underwater robot capable of dynamic payloads," *Int. J. Robot. Res.*, vol. 29, no. 5, pp. 547–570, 2010.

[77] B. Crosbie, M. Anderson, E. Wolbrecht, J. Canning, and D. Edwards, "Synchronous navigation of AUVs using WHOI micro-modem 13-bit communications," in *Proc. OCEANS Conf.*, Sep. 2010, DOI: 10.1109/OCEANS.2010.5664459.

[78] P. Corke, C. Detweiler, M. Dunbabin, M. Hamilton, D. Rus, and I. Vasilescu, "Experiments with underwater robot localization and tracking," in *Proc. IEEE Int. Conf. Robot. Autom.*, Apr. 2007, pp. 4556–4561.

[79] Y. Petillot, F. Maurelli, N. Valeyrie, A. Mallios, P. Ridao, J. Aulinas, and J. Salvi, "Acoustic-based techniques for autonomous underwater vehicle localization," *J. Eng. Maritime Environ.*, vol. 224, pp. 293–307, 2010.

[80] B. Bingham and W. Seering, "Hypothesis grids: Improving long baseline navigation for autonomous underwater vehicles," *IEEE J. Ocean. Eng.*, vol. 31, no. 1, pp. 209–218, Jan. 2006.

[81] E. Olson, J. J. Leonard, and S. Teller, "Robust range-only beacon localization," *IEEE J. Ocean. Eng.*, vol. 31, no. 4, pp. 949–958, Oct. 2006.

[82] A. Bishop, B. Fidan, B. Anderson, K. Dogancay, and P. Pathirana, "Optimal range-difference-based localization considering geometrical constraints," *IEEE J. Ocean. Eng.*, vol. 33, no. 3, pp. 289–301, Jul. 2008.

[83] C. Detweiler, J. Leonard, D. Rus, and S. Teller, "Passive mobile robot localization within a fixed beacon field," in *Proc. 7th Int. Workshop Algorithmic Found. Robot.*, 2006, pp. 1–6.

[84] P. T. Boggs and J. W. Tolle, "Sequential quadratic programming," *Acta Numeric*, pp. 1–52, 1996.

[85] C. Kunz, C. Murphy, H. Singh, C. Pontbriand, R. A. Sohn, S. Singh, T. Sato, C. Roman, K.-I. Nakamura, M. Jakuba, R. Eustice, R. Camilli, and J. Bailey, "Toward extraplanetary under-ice exploration: Robotic steps in the arctic," *J. Field Robot.*, vol. 26, no. 4, pp. 411–429, 2009.

[86] J. Kinsey and L. Whitcomb, "In situ alignment calibration of attitude and Doppler sensors for precision underwater vehicle navigation: Theory and experiment," *IEEE J. Ocean. Eng.*, vol. 32, no. 2, pp. 286–299, Apr. 2007.

[87] D. R. Yoerger, M. Jakuba, A. M. Bradley, and B. Bingham, "Techniques for deep sea near bottom survey using an autonomous underwater vehicle," *Int. J. Robot. Res.*, vol. 26, no. 1, pp. 41–54, 2007.

[88] B. Bingham, "Predicting the navigation performance of underwater vehicles," in *Proc. IEEE/RSJ Int. Conf. Intell. Robots Syst.*, Oct. 2009, pp. 261–266.

[89] C. LaPointe, "Virtual long baseline (VLBL) autonomous underwater vehicle navigation using a single transponder," M.S. thesis, Dept. Mech. Eng., Massachusetts Inst. Technol., Cambridge, MA, USA, 2006.

[90] A. Gadre, "Observability analysis in navigation systems with an underwater vehicle application," Ph.D. dissertation, Dept. Electr. Eng., Virginia Polytech. Inst. State Univ., Blacksburg, VA, USA, 2007.

[91] M. F. Fallon, G. Papadopoulos, J. J. Leonard, and N. M. Patrikalakis, "Cooperative AUV navigation using a single maneuvering surface craft," *Int. J. Robot. Res.*, vol. 29, pp. 1461–1474, 2010.

[92] G. Antonelli, F. Arrichiello, S. Chiaverini, and G. Sukhatme, "Observability analysis of relative localization for AUVs based on ranging and depth measurements," in *Proc. IEEE Int. Conf. Robot. Autom.*, May 2010, pp. 4276–4281.

[93] B. Ferreira, A. Matos, and N. Cruz, "Single beacon navigation: Localization and control of the MARES AUV," in *Proc. OCEANS Conf.*, Sep. 2010, DOI: 10.1109/OCEANS.2010.5664518.

[94] Woods Hole Oceanographic Institution (WHOI), Woods Hole, MA, USA [Online]. Available: http://www.whoi.edu/

[95] Teledyne Technologies, Thousand Oaks, CA, USA [Online]. Available: http://www.teledyne.com/

[96] EvoLogics, Berlin, Germany [Online]. Available: www.evologics.de

[97] E. Gallimore, J. Partan, I. Vaughn, S. Singh, J. Shusta, and L. Freitag, "The WHOI Micromodem-2: A scalable system for acoustic communications and networking," in *Proc. OCEANS Conf.*, Sep. 2010, DOI: 10.1109/OCEANS.2010.5664354.

[98] J. Vaganay, J. Leonard, J. Curcio, and J. Willcox, "Experimental validation of the moving long base-line navigation concept," in *Proc. IEEE/OES Autonom. Underwater Veh. Conf.*, Jun. 2004, pp. 59–65.

[99] A. Matos and N. Cruz, "AUV navigation and guidance in a moving acoustic network," in *Proc. OCEANS Eur. Conf.*, Jun. 2005, vol. 1, pp. 680–685.

[100] S. Webster, R. Eustice, H. Singh, and L. Whitcomb, "Preliminary deep water results in single-beacon one-way-travel-time acoustic navigation for underwater vehicles," in *Proc. IEEE/RSJ Int. Conf. Intell. Robots Syst.*, Oct. 2009, pp. 2053–2060.

[101] S. McPhail and M. Pebody, "Range-only positioning of a deep-diving autonomous underwater vehicle from a surface ship," *IEEE J. Ocean. Eng.*, vol. 34, no. 4, pp. 669–677, Oct. 2009.

[102] A. Folk, B. Armstrong, E. Wolbrecht, H. Grip, M. Anderson, and D. Edwards, "Autonomous underwater vehicle navigation using moving baseline on a target ship," in *Proc. OCEANS Conf.*, Sep. 2010, DOI: 10.1109/OCEANS.2010.5664462.

[103] R. Eustice, L. Whitcomb, H. Singh, and M. Grund, "Experimental results in synchronous-clock one-way-travel-time acoustic navigation for autonomous underwater vehicles," in *Proc. IEEE Int. Conf. Robot. Autom.*, Apr. 2007, pp. 4257–4264.

[104] R. M. Eustice, H. Singh, and L. L. Whitcomb, "Synchronous-clock, one-way-travel-time acoustic navigation for underwater vehicles," *J. Field Robot.*, vol. 28, no. 1, pp. 121–136, 2011.

[105] A. Bahr and J. J. Leonard, "Cooperative localization for autonomous underwater vehicles," in *Proc. Int. Symp. Exp. Robot.*, 2006, pp. 1–10.

[106] G. Papadopoulos, M. Fallon, J. Leonard, and N. Patrikalakis, "Cooperative localization of marine vehicles using nonlinear state estimation," in *Proc. IEEE/RSJ Int. Conf. Intell. Robots Syst.*, Oct. 2010, pp. 4874–4879.

[107] M. Chitre, "Path planning for cooperative underwater range-only navigation using a single beacon," in *Proc. Int. Conf. Autonom. Intell. Syst.*, Jun. 2010, DOI: 10.1109/AIS.2010.5547044.

[108] D. Viegas, P. Batista, P. Oliveira, and C. Silvestre, "Position and velocity filters for intervention AUVs based on single range and depth measurements," in *Proc. IEEE Int. Conf. Robot. Autom.*, May 2012, pp. 4878–4883.

[109] F. Arrichiello, H. Heidarsson, and G. Sukhatme, "Opportunistic localization of underwater robots using drifters and boats," in *Proc. IEEE Int. Conf. Robot. Autom.*, May 2012, pp. 5307–5314.

[110] Liquid Robotics, Sunnyvale, CA, USA [Online]. Available: liquidr.com

[111] B. Bingham, N. Kraus, B. Howe, L. Freitag, K. Ball, P. Koski, and E. Gallimore, "Passive and active acoustics using an autonomous wave glider," *J. Field Robot.*, vol. 29, no. 6, pp. 911–923, 2012.

[112] G. Rui and M. Chitre, "Cooperative positioning using range-only measurements between two AUVs," in *Proc. IEEE OCEANS Conf.*, May 2010, DOI: 10.1109/OCEANSSYD.2010.5603615.

[113] A. Bahr, J. J. Leonard, and M. F. Fallon, "Cooperative localization for autonomous underwater vehicles," *Int. J. Robot. Res.*, vol. 28, no. 6, pp. 714–728, Jun. 2009.

[114] A. Bahr, M. Walter, and J. Leonard, "Consistent cooperative localization," in *Proc. IEEE Int. Conf. Robot. Autom.*, May 2009, pp. 3415–3422.

[115] A. Bahr, "Cooperative localization for autonomous underwater vehicles," Ph.D. dissertation, Joint Program Appl. Ocean Sci. Eng., Massachusetts Inst. Technol., Cambridge, MA, USA, 2009.

[116] M. Dunbabin, P. Corke, I. Vasilescu, and D. Rus, "Experiments with cooperative control of underwater robots," *Int. J. Robot. Res.*, vol. 28, no. 6, pp. 815–833, 2009.

[117] D. Maczka, A. Gadre, and D. Stilwell, "Implementation of a cooperative navigation algorithm on a platoon of autonomous underwater vehicles," in *Proc. OCEANS Conf.*, Oct. 2007, DOI: 10.1109/OCEANS.2007.4449404.

[118] M. Fallon, G. Papadopoulos, and J. Leonard, "A measurement distribution framework for cooperative navigation using multiple AUVs," in *Proc. IEEE Int. Conf. Robot. Autom.*, May 2010, pp. 4256–4263.

[119] B. Armstrong, E. Wolbrecht, and D. Edwards, "AUV navigation in the presence of a magnetic disturbance with an extended Kalman filter," in *Proc. IEEE OCEANS Conf.*, May 2010, DOI: 10.1109/OCEANSSYD.2010.5603905.

[120] B. Armstrong, J. Pentzer, D. Odell, T. Bean, J. Canning, D. Pugsley, J. Frenzel, M. Anderson, and D. Edwards, "Field measurement of surface ship magnetic signature using multiple AUVs," in *Proc. MTS/IEEE OCEANS Conf.*, Oct. 2009, pp. 1–9.

[121] D. G. Lowe, "Object recognition from local scale-invariant features," in *Proc. IEEE Int. Conf. Comput. Vis.*, Aug. 1999, vol. 2, pp. 1150–1157.

[122] H. Bay, A. Ess, T. Tuytelaars, and L. Van Gool, "Speeded-up robust features (SURF)," *Comput. Vis. Image Understand.*, vol. 110, pp. 346–359, Jun. 2008.

[123] K. Mikolajczyk, T. Tuytelaars, C. Schmid, A. Zisserman, J. Matas, F. Schaffalitzky, T. Kadir, and L. Gool, "A comparison of affine region detectors," *Int. J. Comput. Vis.*, vol. 65, no. 1, pp. 43–72, Nov. 2005.

[124] A. Kim and R. Eustice, "Pose-graph visual SLAM with geometric model selection for autonomous underwater ship hull inspection," in *Proc. IEEE/RSJ Int. Conf. Intell. Robots Syst.*, Oct. 2009, pp. 1559–1565.

[125] I. Mahon, S. Williams, O. Pizarro, and M. Johnson-Roberson, "Efficient view-based SLAM using visual loop closures," *IEEE Trans. Robot.*, vol. 24, no. 5, pp. 1002–1014, Oct. 2008.

[126] F. S. Hover, R. M. Eustice, A. Kim, B. Englot, H. Johannsson, M. Kaess, and J. J. Leonard, "Advanced perception, navigation and planning for autonomous in-water ship hull inspection," *Int. J. Robot. Res.*, vol. 31, no. 12, pp. 1445–1464, 2012.

[127] A. Kim and R. M. Eustice, "Real-time visual SLAM for autonomous underwater hull inspection using visual saliency," *IEEE Trans. Robot.*, vol. 29, no. 3, pp. 719–733, Jun. 2013.

[128] H. Singh, C. Roman, O. Pizarro, R. Eustice, and A. Can, "Towards high-resolution imaging from underwater vehicles," *Int. J. Robot. Res.*, vol. 26, no. 1, pp. 55–74, 2007.

[129] M. Johnson-Roberson, O. Pizarro, S. B. Williams, and I. Mahon, "Generation and visualization of large-scale three-dimensional reconstructions from underwater robotic surveys," *J. Field Robot.*, vol. 27, no. 1, pp. 21–51, 2010.

[130] M. Pfingsthorn, A. Birk, and H. Bulow, "An efficient strategy for data exchange in multi-robot mapping under underwater communication constraints," in *Proc. IEEE/RSJ Int. Conf. Intell. Robots Syst.*, Oct. 2010, pp. 4886–4893.

[131] J. Diosdado and I. Ruiz, "Decentralised simultaneous localisation and mapping for AUVs," in *Proc. OCEANS Eur. Conf.*, Jun. 2007, DOI: 10.1109/OCEANSE.2007.4302397.

[132] A. Ortiz, J. Antich, and G. Oliver, "A Bayesian approach for tracking undersea narrow telecommunication cables," in *Proc. OCEANS Eur. Conf.*, May 2009, DOI: 10.1109/OCEANSE.2009.5278108.

[133] I. T. Ruiz, S. de Raucourt, Y. Petillot, and D. Lane, "Concurrent mapping and localization using sidescan sonar," *IEEE J. Ocean. Eng.*, vol. 29, no. 2, pp. 442–456, Apr. 2004.

[134] L. Jaulin, "A nonlinear set membership approach for the localization and map building of underwater robots," *IEEE Trans. Robot.*, vol. 25, no. 1, pp. 88–98, Feb. 2009.

[135] J. Aulinas, A. Fazlollahi, J. Salvi, X. Llado, Y. Petillot, J. Sawas, and R. Garcia, "Robust automatic landmark detection for underwater SLAM using side-scan sonar imaging," in *Proc. 11th Int. Conf. Mobile Robots Competitions*, Lisboa, Portugal, Apr. 2011, pp. 21–26.

[136] H. Johannsson, M. Kaess, B. Englot, F. Hover, and J. Leonard, "Imaging sonar-aided navigation for autonomous underwater harbor surveillance," in *Proc. IEEE/RSJ Int. Conf. Intell. Robots Syst.*, Oct. 2010, pp. 4396–4403.

[137] G. Shippey, M. Jonsson, and J. Pihl, "Position correction using echoes from a navigation fix for synthetic aperture sonar imaging," *IEEE J. Ocean. Eng.*, vol. 34, no. 3, pp. 294–306, Jul. 2009.

[138] F. Sun, W. Xu, and J. Li, "Enhancement of the aided inertial navigation system for an AUV via micronavigation," in *Proc. OCEANS Conf.*, Sep. 2010, DOI: 10.1109/OCEANS.2010.5664097.

[139] P. M. Newman, J. J. Leonard, and R. J. Rikoski, "Towards constant-time SLAM on an autonomous underwater vehicle using synthetic aperture sonar," in *Proc. 11th Int. Symp. Robot. Res.*, 2003, pp. 409–420.

[140] A. Mallios, P. Ridao, E. Hernandez, D. Ribas, F. Maurelli, and Y. Petillot, "Pose-based SLAM with probabilistic scan matching algorithm using a mechanical scanned imaging sonar," in *Proc. OCEANS Eur. Conf.*, May 2009, DOI: 10.1109/OCEANSE.2009.5278219.

[141] A. Mallios, P. Ridao, D. Ribas, and E. Hernandndez, "Probabilistic sonar scan matching SLAM for underwater environment," in *Proc. IEEE OCEANS Conf.*, May 2010, DOI: 10.1109/OCEANSSYD.2010.5603650.

[142] A. Mallios, P. Ridao, D. Ribas, F. Maurelli, and Y. Petillot, "EKF-SLAM for AUV navigation under probabilistic sonar scan-matching," in *Proc. IEEE/RSJ Int. Conf. Intell. Robots Syst.*, Oct. 2010, pp. 4404–4411.

[143] E. Hernandez, P. Ridao, D. Ribas, and A. Mallios, "Probabilistic sonar scan matching for an AUV," in *Proc. IEEE/RSJ Int. Conf. Intell. Robots Syst.*, Oct. 2009, pp. 255–260.

[144] N. Fairfield, G. Kantor, D. Jonak, and D. Wettergreen, "Autonomous exploration and mapping of flooded sinkholes," *Int. J. Robot. Res.*, vol. 29, no. 6, pp. 748–774, 2010.

[145] N. Fairfield, G. Kantor, and D. Wettergreen, "Real-time SLAM with octree evidence grids for exploration in underwater tunnels," *J. Field Robot.*, vol. 24, no. 1-2, pp. 03–21, 2007.

[146] T. Maki, H. Kondo, T. Ura, and T. Sakamaki, "Imaging vent fields: SLAM based navigation scheme for an AUV toward large-area seafloor imaging," in *Proc. IEEE/OES Autonom. Underwater Veh. Conf.*, Oct. 2008, DOI: 10.1109/AUV.2008.5290530.

[147] W. J. Kirkwood, "Development of the DORADO mapping vehicle for multibeam, subbottom, and sidescan science missions," *J. Field Robot.*, vol. 24, no. 6, pp. 487–495, 2007.

[148] J. Aulinas, X. Llado, J. Salvi, and Y. Petillot, "Selective submap joining for underwater large scale 6-DOF SLAM," in *Proc. IEEE/RSJ Int. Conf. Intell. Robots Syst.*, Oct. 2010, pp. 2552–2557.

[149] P. Woock, "Survey on suitable 3D features for sonar-based underwater navigation," in *Proc. OCEANS Conf.*, May 2012, DOI: 10.1109/OCEANS-Yeosu.2012.6263449.

[150] H. Bülow and A. Birk, "Spectral registration of noisy sonar data for underwater 3D mapping," *Autonom. Robots*, vol. 30, pp. 307–331, Apr. 2011.

[151] M. Pfingsthorn, A. Birk, and H. Bulow, "Uncertainty estimation for a 6-DOF spectral registration method as basis for sonar-based underwater 3D SLAM," in *Proc. IEEE Int. Conf. Robot. Autom.*, 2012, pp. 3049–3054.

[152] K. Pathak, A. Birk, and N. Vaskevicius, "Plane-based registration of sonar data for underwater 3D mapping," in *Proc. IEEE/RSJ Int. Conf. Intell. Robots Syst.*, Oct. 2010, pp. 4880–4885.

Sajad Saeedi received the B.Eng. degree in electrical engineering from K. N. Toosi University of Technology, Tehran, Iran, in 2001 and the M.S. degree in electrical engineering from Tarbiat Modares University, Tehran, Iran, in 2004.

His research interests include simultaneous localization and mapping, multiagent systems, path planning, intelligent systems, and nonlinear control.

Mae Seto received the B.A.Sc. degree in engineering physics—electrical and the Ph.D. degree in mechanical engineering from the University of British Columbia, Vancouver, BC, Canada, in 1987 and 1996, respectively.

She is a Senior Defence Scientist at the Defence R&D Canada, Dartmouth, NS, Canada and Leader of the Mine and Harbour Defence Group. She is also an Adjunct Professor of Mechanical Engineering and Computer Science at Dalhousie University, Halifax, NS, Canada and the University of New Brunswick, Fredericton, NB, Canada. Her research interests include intelligent autonomy for marine autonomous vehicles and systems, underwater vehicle and tow body dynamics, multiagent systems, and underwater acoustics. She has published numerous papers in these areas.

Dr. Seto was an NSERC Industrial Postdoctoral Fellow doing research on autonomous underwater vehicles and unmanned surface vehicles.

Howard Li received the Ph.D. degree in electrical and computer engineering from the University of Waterloo, Waterloo, ON, Canada.

He is an Associate Professor in the Department of Electrical and Computer Engineering, University of New Brunswick, Fredericton, NB, Canada. He also worked for Atlantis Systems International, Defence Research and Development Canada, and Applied AI Systems Inc. to develop unmanned ground vehicles, unmanned aerial vehicles, autonomous underwater vehicles, and mobile robots for both domestic and military applications. His research interests include linear control, nonlinear control, intelligent control, distributed control, unmanned vehicles, mechatronics, robotics, multiagent systems, artificial intelligence, motion planning, and simultaneous localization and mapping.

Prof. Li is a registered Professional Engineer in the Province of Ontario, Canada.

Liam Paull received the B.Eng. degree in computer engineering from McGill University, Montreal, QC, Canada, in 2004. He began the M.Sc. degree in electrical engineering at the University of New Brunswick, Frederickton, NB, Canada, in 2007 and then transitioned to a Ph.D. program in electrical engineering in 2008.

His research interests include: autonomous underwater vehicle planning and navigation, cooperative localization, multiagent systems, and simultaneous localization mapping.